HIGHLIGHTS AND ACTIVITIES 2011-2012

MAX IV LABORATORY

CONTENTS

Front cover photograph:
A sample surrounded by eight electromagnets in the octupole end station at beamline I1011.

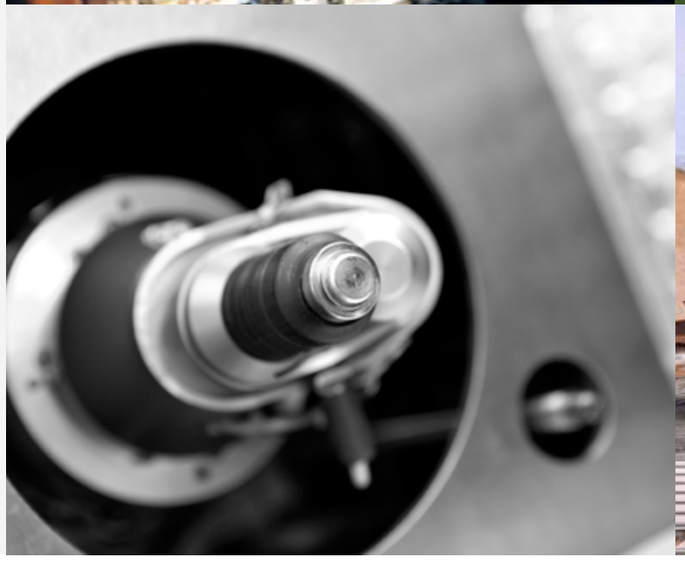

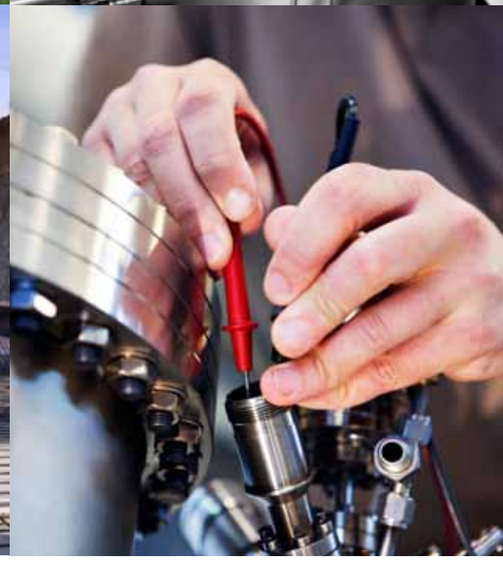

INTRODUCTION BY THE DIRECTOR

Dear Reader

The *Highlights and Activities 2011-2012* report is the successor of the MAX-lab Activity Reports. A major component of the Activity Reports was the user reports on experiments performed at MAX-lab during the year, which gave the reader detailed insight into the MAX-lab user programme. Similar to previous years the laboratory has assembled reports on user experiments performed in 2011, which are available on the laboratory website. Some of these are presented in the *Scientific Highlights* section of this report and serve to illustrate the wide scientific range of the research performed at the three MAX-lab rings.

The change in content and layout of the annual report from the laboratory has been initiated by changes implemented by the agreement on the MAX IV Laboratory signed in 2010 by the funders (Swedish Research Council, VINNOVA, Lund University and Region Skåne) of the MAX IV project, where MAX-lab became a part of the MAX IV Laboratory. The agreement was accompanied by significant changes in the organisational structure that have been fully implemented during 2011. The appointment of Peter Andersson as Administrative Director in August 2011 completed the management team comprised of the four directors. The new organisation of the laboratory is described in greater detail in *This is the MAX IV Laboratory* and the *Facts and Figures* section.

For the MAX IV Laboratory it is easy to identify the most important events that took place during 2011 and 2012. The first is the start of the construction of the MAX IV linac building at Brunnshög in May 2011, after Lund University had signed a preliminary leasing contract with the company ML4. Shortly thereafter, in June 2011, the plans for the exterior of the MAX IV buildings were presented. The construction of the MAX IV facility is progressing rapidly as described in the section *The MAX IV Building Project*. The second very important event took place when funding was obtained from the Knut and Alice Wallenberg Foundation (KAW) and 12 Swedish Universities that will enable the construction of the first seven beamlines at MAX IV, see the section *The MAX IV Beamlines*. This funding is a result of a major effort by Science Director Jesper Andersen and his project team, who prepared the 747 page application submitted to KAW in May 2011. Co-financing by at least 25% from other sources was a condition for obtaining the 400 MSEK grant from KAW. It made me personally very happy and cemented the role of the MAX IV Laboratory as a national laboratory when 12 of the larger Swedish universities decided to provide the additional funding of 162 MSEK to the beamline projects. The official letter on the funding from KAW was received in the summer of 2011 and since then much progress has been achieved in the seven beamline projects, in which scientists from many of the Swedish universities are engaged. In order to stimulate and secure the contacts to Swedish universities a special University Reference Group has been created with representatives from the 12 universities.

These developments, accompanied by organisational changes, stimulated a quest for a renewed and stronger visual identity. During 2011 a new logo was developed and subsequently approved by the MAX IV Laboratory Board and Lund University. The logo with the two circles that illustrate the two rings of MAX IV is an important component in the new website and underlines the layout of the present publication.

On the European synchrotron scene MAX-lab was known as a small and well-functioning facility. With the MAX IV project the laboratory has attracted significant international attention. It would not be possible to realize the MAX IV project without the valuable collaborations with other facilities all over the world. To mention a few, the Polish synchrotron SOLARIS will be a copy of the small 1.5 GeV ring of MAX IV and the collaboration with the SOLARIS team is of great mutual benefit. The collaboration contract between the Swedish Research Council and the French synchrotron SOLEIL, which involves the MAX IV Laboratory, was signed at the end of 2011, see *This is the MAX IV Laboratory*. Many valuable areas for collaboration between SOLEIL and the MAX IV Laboratory have already been identified in particular with respect to the construction of beamlines.

Good and constructive interactions with the Users organisation FASM are vital for the continued operation of MAX-lab and the development of the beamline programme for MAX IV. I would like to use this opportunity to thank FASM for their dedicated work and the users of MAX-lab for their support.

This report contains details on the activities of the present MAX-lab and the MAX IV project, but in the Scientific Highlight *FEL – Tests Today and Outlook for Tomorrow* there is also a vision for the development of the MAX IV Laboratory beyond 2020. Free Electron Laser (FEL) projects are under realisation at several places worldwide, and to keep the position as a leading photon source it is important that the MAX IV Laboratory is part of this development on a national and European basis. Considering the resources available for the development of photon science in Sweden, I considered it as a special Christmas present when FEL Center Stockholm-Uppsala, Uppsala University, Lund Laser Center and the MAX IV Laboratory in December 2011 agreed to work together on the development of FEL science in Sweden.

The MAX IV project really took off during 2011, and very importantly without any negative effects on the operation of MAX-lab. This progress would not have been possible without the support from the host institution Lund University and the other funders the Swedish Research Council, VINNOVA and Region Skåne, and last but not least by the hard and dedicated work of the staff of the MAX IV Laboratory. Therefore on behalf of the Management team I would like to express my warmest thanks to the staff and the funders of the MAX IV Laboratory. ■

Sine Larsen
Director MAX IV Laboratory
2011-2012

THIS IS THE MAX IV LABORATORY

The MAX IV Laboratory was established in July 2010 as a Swedish, national laboratory hosted by Lund University. It is the successor of the national laboratory MAX-lab and includes both the operation of the present MAX-lab (MAX I, II, and III rings) and the MAX IV project under realization at Brunnshög in the north-eastern part of Lund.

Photographer: Perry Nordeng

The formal goals and basic governance of the MAX IV Laboratory were established in an agreement between Lund University (LU), the Swedish Research Council (VR) and VINNOVA in June 2010 and by a related agreement between Lund University and Region Skåne (RS) in July 2010. The agreement between LU, VR and VINNOVA specifies the governing organisation of the MAX IV Laboratory, the role and composition of the Board, the structure of the operative management team and the financing of the construction of the new MAX IV facility.

LU, VR, VINNOVA and RS have also established an informal coordinating forum "Forum for Funders", comprised of representatives of these organisations. The Chairperson of the Board of the MAX IV Laboratory chairs the Forum. The Forum will provide the funders with information on the progress of the MAX IV project, offer opportunities for discussion of the overall strategic preconditions for MAX IV and provide a platform for the coordination of possible actions. The memberships of the governing bodies are listed in the Facts and Figures section of this report.

The agreement on the MAX IV Laboratory in 2010 has been accompanied by significant changes in the organisation and management of the laboratory during 2011 and 2012. To meet the challenges of the new MAX IV project a thorough process to reinforce the human resources and administrative procedures was initiated.

The present MAX IV Laboratory is based on MAX-lab's more than 25 years of experience in accelerator physics and storage ring based research. MAX IV, which will be a synchrotron radiation facility with an outstanding performance, is built on this experience. Today about 140 people are employed and the laboratory further benefits by hosting staff from two divisions at Lund University (Division for Accelerator Physics and Division for Synchrotron Radiation Instrumentation) forming the MAX N-fak unit.

MAX-lab is privileged by having a continuously growing and active user community across a wide range of sciences that since 1985 has contributed to the development of the laboratory. The user community is also heavily engaged in the MAX IV project, which when completed in 2016 will be able to provide researchers a high level of service at one of the world's most advanced synchrotron light sources.

The MAX IV Project

MAX IV is comprised of two storage rings and one linear accelerator. The circumference of the 3 GeV ring will be 528 meters and it will be the most brilliant synchrotron light source in the world. It will provide the Swedish, Scandinavian and international scientific communities unique opportunities for experiments. The large 3 GeV ring will be complemented by a smaller 1.5 GeV ring for experiments using light in the lower energy part of the spectrum and both rings will be injected by a linear accelerator with a full length of 250 meters. The MAX IV project is described in greater details in the following chapters.

The construction of the MAX IV accelerators and accompanying infrastructure is financed by the Swedish Research Council, Lund University, VINNOVA, and Region Skåne. The construction is proceeding on schedule with the installation of the linear accelerator planned to start in May 2013. The installation of the 3 GeV ring should commence in April 2014 while the 1.5 GeV ring installation will start six months later.

Funding for the first seven beamlines has been provided by the Knut and Alice Wallenberg Foundation and a joint initiative of Swedish universities. The MAX IV facility can accommodate a total of 30 beamlines and the present funding enables construction of beamlines for about 25% of this capacity.

The collaborations with other synchrotron facilities in the world are essential for the realization of the project, due to the very limited staff at the MAX IV Laboratory. During 2011 several agreements with other facilities were signed for example with SOLEIL.

The present MAX-lab

Since the 1980's, MAX-lab has supported three distinct research areas: Accelerator Physics, research based on the use of Synchrotron Radiation and Nuclear Physics using energetic electrons. The time for measurements at the facility is shared between these three areas; see the *Scientific Highlights* for more information.

A strong engagement of the user community is and has been essential in the development of MAX-lab. The laboratory has likewise been important for the development of Swedish front-line positions in several areas of synchrotron radiation based research. This synergetic facility-community relation will be maintained for an optimum development of the MAX IV facility. ■

Figure 1.
SOLEIL Director Jean Daillant signing the agreement between the Swedish Research Council and SOLEIL on 21 December 2011

Figure 2.
Four generations of MAX-lab/MAX IV Laboratory directors. From left to right: Sine Larsen, Nils Mårtensson, Ingolf Lindau and Bengt Forkman.

Figure 1 - 3 .
Different stages in the construction of the MAX IV linac tunnel:
1. Excavation in August 2011.

2. Assembly of the steel reinforcement bars for the slab and walls in September 2011.

3. The klystron gallery in June 2012.

THE MAX IV BUILDING PROJECT

2011 stands as an extremely important year for the construction of the MAX IV facility. The overall start of construction work started in May with preparatory groundwork. The construction of the first structures, including the linac accelerator tunnel, soon commenced in June 2011. As of August 2012, the linac tunnel is nearing completion while the construction of the foundations for the 3 GeV ring is progressing at a steady pace.

MAX IV is currently being constructed at Brunnshög in north-eastern Lund. The construction site is located on land owned by the City of Lund between the motorway E22 and Odarslövsvägen.

The MAX IV construction work is carried out by the contracting company PEAB AB on commission of the future owner, Fastighets AB ML4 (ML4), which was formed in 2010 by PEAB and the real estate company Wihlborg AB for the sole purposes of building and maintaining the MAX IV building complex. As Swedish universities are not allowed to own buildings, all MAX IV buildings will be owned by ML4, which will lease them to Lund University and the MAX IV Laboratory when they are completed.

A goal is to make MAX IV a sustainable research facility, probably the first in the world of its kind, with accelerators and all technical equipment designed for lowest reasonable power use. The buildings will be designed for energy efficiency and the equipment will be operated using intelligent power management. Electrical power will be bought from renewable sources and the excess heat from the cooling systems will be sold and used in the Lund city district heating and cooling system. The aim is to have a power consumption that corresponds to approximately 50% of similar facilities.

Figure 4.
Aerial rendering of the MAX IV exterior architecture and landscaping by FOJAB and Snøhetta. South-west is towards the top of the image.

After a prequalification phase, four architect firms (3xN, FOJAB, Grimshaw and Snøhetta) were chosen in 2010 to develop ideas for the external design of the building and the landscape around it. The four proposals were all deemed interesting, but a jury consisting of representatives from Lund University, Lund municipality building office and ML4 finally recommended that FOJAB should work on the design of the buildings while Snøhetta should be responsible for the landscape design. The aim is to build a facility that will serve the science well, be environmentally friendly and be an eye catcher in the dynamic north-eastern Lund area.

Early diggings were made in 2010 to test some stabilizing construction solutions (see the following chapter: *The Stability of MAX IV*). Both ML4 and the MAX IV Laboratory were heavily engaged in work for the preparation of the construction site, which was officially inaugurated in the presence of the Swedish Deputy Prime Minister and Minister for Education Jan Björklund on the 22 November 2010.

The building project is divided into two stages. The first stage includes the building of the 300 meter long linear accelerator tunnel, the linac start building, the SPF-facility and technical support buildings while the second stage includes the erection of the main ring buildings and the office building.

After the signing of a preliminary rental agreement for Stage 1 between Lund University and ML4 the first proper construction work could finally begin in May 2011.

The linac tunnel and the connected klystron gallery is a particularly important project milestone. The tunnels consist of thick concrete walls that had to be cast with extremely high precision. During the casting of the tunnel up to 20 cubic meters of concrete was delivered to the site every hour. The onsite concrete construction of the linac tunnel walls was completed in August 2012 with only a small part of the tunnel roof remaining. Figure 1 to 3 shows the development of the construction of the linac tunnel.

Year 2012 also saw the start of the installation and finishing works in the tunnels such as electrical installations, painting of the walls and polishing of the floor, which will pave way for the assembly of the linac commencing in May 2013. Commissioning of the accelerator will follow during 2014 with full operation planned for the first quarter of 2015.

The work with the landscaping continued during 2011. GPS equipped bulldozers, programmed exactly according to the landscape designer's instructions, moulded the heights and slopes that will surround the facility. Hence the fertile soil will not be removed from the site, but reused as vibrations reduction and a landscape feature.

During Stage 2, buildings above ground including the 1.5 GeV and 3 GeV rings, and the office building will be constructed. These structures can be seen in the overall design of the MAX IV complex (shown in Figure 4) as presented by the architects in June 2011.

Stage 2 started in the summer of 2012. Approximately one-quarter of the 4 meter thick layer of lime stabilised soil upon which the 3 GeV ring building will rest has been completed as of August 2012. The building will be ready for installation of the 3 GeV ring in April 2014 with commissioning during 2015 and full operation in 2016. The 1.5 GeV ring building will be completed 6 months after the larger ring.

The aerial view in Figure 7 shows the MAX IV construction site in August 2012. It is a huge work place and since spring 2012 between 150 and 200 persons work there every day. From autumn 2013 to spring 2014 it is expected that more than 400 persons will be working at the construction site. The construction works is planned to be finished in late 2015. ■

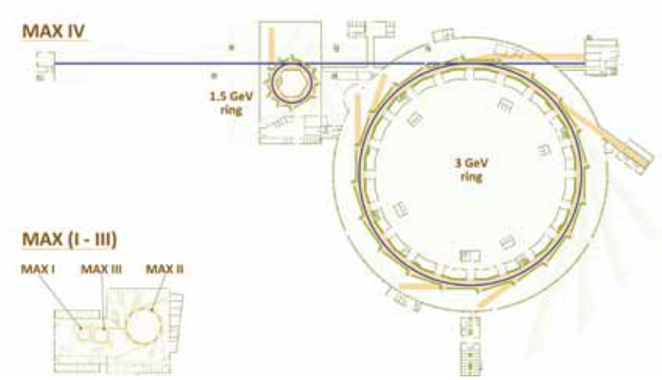

Figure 5.
Comparison between the MAX IV facility and MAX-lab.

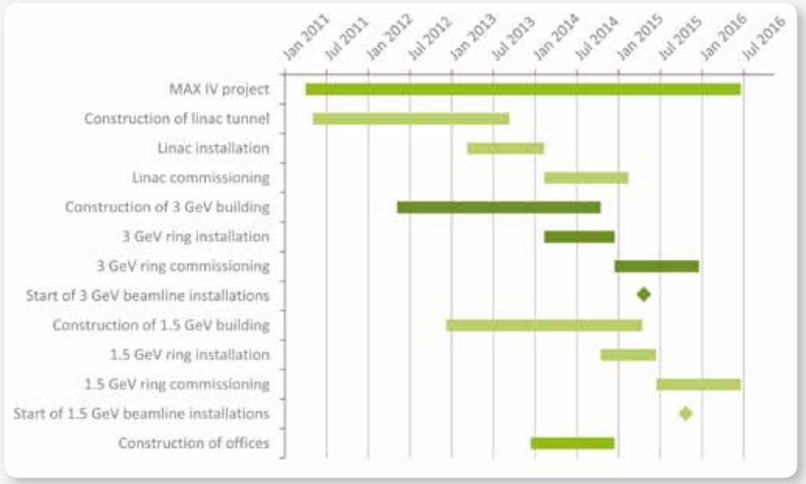

Figure 6.
Gantt-chart showing the main sub-projects and milestones in the MAX IV project.

Figure 7.
The MAX IV construction site in August 2012. south-east is towards the top of the image.

Photographer: Perry Nordeng

THE STABILITY OF MAX IV

Brian Norsk Jensen
MAX IV Laboratory, Lund University, Sweden

Vibrations of the accelerator and storage ring components may influence the performance of MAX IV. A lot of effort has therefore been made to ensure the facility's stability towards vibrations from the nearby motorway and other sources. Solutions include a 4 meter thick Lime Stabilized Soil (LSS) layer supporting the facility and tailor made hills in the landscape surrounding the buildings. An overall theme for the stability work is cost efficiency following the MAX-lab tradition of finding new and unconventional solutions to problems.

In order to guarantee the exceptional performance of MAX IV it is important that vibrations can be reduced. For this purpose some specific goals have been set for the stability of the facility. The overall stability goal is defined by the size of the electron beam and its behaviour when the accelerator components are vibrating.

The MAX IV Laboratory and ML4 have collaborated since 2010 on finding a cost effective civil engineering concept to ensure an acceptable level of vibrations. The work has been performed by a multidisciplinary group of civil engineers, geophysicists and other specialists who have worked in unison to find an optimal solution.

The geophysical conditions at the Brunnshög site have been investigated thoroughly using various methods. Different seismic investigations have been performed and resistivity measurements were carried out across the whole area of the MAX IV site to identify different layers in the soil. Samples of the soil and bedrock have been extracted by drilling and then analysed by geologists and geophysicists.

The results of the various measurements formed the base for very large Finite Element Method (FEM) calculations performed during the project. A mock-up model has also been built to test the idea for the foundation. This work resulted in the solution of using a 4 meter layer of LSS as the main structural part of the foundation for all buildings above ground.

The LSS solution fits very well with the relatively stiff clay till at the MAX IV site. The method is in addition environmentally friendly since it helps to reduce the amount of soil that otherwise has to be deposited elsewhere, and it is also very cost efficient when it comes to reaching a certain degree of stiffness of the foundation. The method is not new however, since it was used already by the Romans for road building.

The MAX IV Laboratory is collaborating with the Department of Construction Sciences at LTH and several students from the department have written their master theses on topics related to MAX IV and its stability. One of the students investigated the effect of varying the shape of the landscape surrounding MAX IV. The calculations showed that this could have a reductive effect on vibrations coming from the outside and it animated the architects to come up with the idea for the hill pattern for the MAX IV surroundings. More detailed investigations are needed, but the preliminary results show a possibility of vibration reduction in the area of 20% by an 80 meter wide "bumpy field" of hills. The explanation is that the refractive index in the soil for the vibration waves is varied by the bumps and the transmitted vibrations are then reduced by elastic scattering. Other research by students have been done on the effect of a local road originally planned to cross the linac tunnel and the effect of traffic crossing a tunnel for this road under the motorway E22.

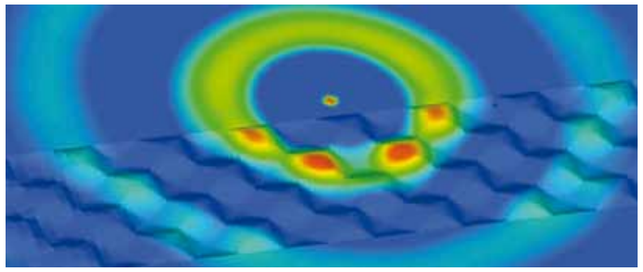

Figure 1.
Wave propagation through a bumpy landscape. Picture: Per Jørstad.

Several larger and smaller projects are currently on-going at MAX IV Laboratory in the field of stability. A project on "Stable Supports" for MAX IV has been going on for some time. The objective for the project is the development of stands and supports to make sure that we are taking full advantage of the stable floors of the facility. The surveyors at MAX IV are involved in the project to make sure that the solutions ensure stability as well as optimal alignment conditions. Prototypes have been made and tested for some of the vital supports in order to confirm the results from FEM calculations.

Another project is on "Passive Vibration Isolation". The main objective here is to isolate vibration sources, for example vacuum pumps. Passive isolation of pulsations in cooling water is an area we are working on partly together with consultants for the landlord ML4, both on a larger scale for the main supply of cooling water and for local very small solutions for cooling of optical components.

Temperature fluctuations may lead to thermal expansion of sensitive facility components and their supports and hence influence the performance of MAX IV. The quality of optical components may also degrade if cooling is not sufficient or stable enough. Thermal stability of both the cooling water for the facility components and of the air in beamline hutches is being discussed and solutions are emerging for different grades of stability.

An overall theme for all the work is that we have to solve the challenges in a cost efficient manner. This is following the tradition at MAX-lab of finding new and sometimes even unconventional solutions.

The MAX IV Laboratory is now taking over the seismometers that have been used at the MAX IV site for green field vibration measurements and geotechnical characterization. The plan is to use these devices to create a system for continuous monitoring of the running facility. Such a system will be used to identify emerging vibration problems, new sources etc. A similar system for monitoring cooling water pulsations should be a part of this project.

For further reading on stability at the MAX IV see:
https://www.maxlab.lu.se/node/1226

THE MAX IV ACCELERATOR PROJECT

Pedro Fernandes Tavares and Mikael Eriksson
MAX IV Laboratory, Lund University, Sweden

The MAX IV accelerator project proceeds according to the time-schedule. The year 2011 marked a decisive turning point, as the focus of the project team shifted from conceptual design and preparation work to actual detailed engineering design, procurement and fabrication of components for the various subsystems in the three accelerators that make up the MAX IV facility. As of August 2012, close to half of the machine equipment has been ordered. To cope with the relatively lean staff organisation, an extensive cooperation program has been started with other accelerator laboratories like Budker Institute of Nuclear Physics, SOLEIL, PSI, CERN, ALBA, Solaris and CLS. The MAX IV Laboratory Machine Advisory Committee (MAC) plays an important advising role.

Early proposals for building a new state-of-the-art synchrotron light source to replace the existing MAX-lab rings date back to before year 2000. The scientific case and technical design have since then been developed in detail and the project has obtained decisive support from funding agencies and the Swedish and Scandinavian scientific communities.

Funding obtained from the Knut and Alice Wallenberg foundation in 2006 enabled the preparation of a Detailed Design Report by the MAX-lab team, proposing a facility based on a suite of machines each focusing on different user needs, ranging in wavelengths from infra-red to hard X-rays as well as very short X-ray pulse durations. As a result of interactions with the user community and scrutiny by the MAC (see Facts and Figures), the design evolved from a concept of two rings sharing the same tunnel to a design with two rings of different circumferences.

The current solution with one ring operating at 1.5 GeV optimized for softer radiation and a larger 3 GeV ring providing ultra-low emittance and hence ultra-high brightness up to the hard X-ray region uses various innovative concepts. The MAX IV concept to achieve an electron beam of very high quality implies compact magnets machined out of common iron blocks, NEG coated vacuum chambers and a 100 MHz RF system. These technical solutions result in an unprecedented performance (see Figure 4 and Table 1) in a relatively small ring circumference and at a low cost compared to conventional concepts.

The facility is complemented by a full energy linear accelerator (linac), which not only provides electrons for filling both rings in top-up mode, but will also be able to generate very short X-ray pulses by spontaneous emission in undulators comprising the Short Pulse Facility (SPF). The linac design has been prepared for future upgrades into a free electron laser (FEL) to meet the growing needs of extremely short and intense X-ray pulses of the user community.

Funding for the construction of MAX IV from the Swedish Research Council (VR), Lund University, VINNOVA and Region Skåne was officially announced in 2010 which allowed the effective start of the project.

Updates on the progress of the MAX IV accelerator project

Linac
The construction of the injector linac building and the procurement and delivery of linac components proceeds as planned. The main items for the linac have been ordered: 18 RF stations, 40 five meter long accelerating sections with their SLED cavities, diagnostics, vacuum parts and magnet systems. All of the RF stations have been manufactured and have passed the factory acceptance test. One of these RF stations has been shipped to Bonn in Germany to be used for the linac structure and SLED cavity conditioning just starting up there.

A linac injector test-stand has been constructed at MAX-lab. Several RF guns have been produced; a laser-cathode gun intended for the Short Pulse Facility as well as the thermionic gun to be used for injection into the rings. These guns are currently being characterized and conditioned prior to the linac installation at Brunnshög. Installation in the linac building is planned to commence in May 2013.

Storage Ring Magnets
A major milestone in the manufacturing of storage ring magnets was the signature of fabrication contracts for all the 140 magnet blocks for the 3 GeV storage ring.

Figure 1.
Details from the linac injector test stand.

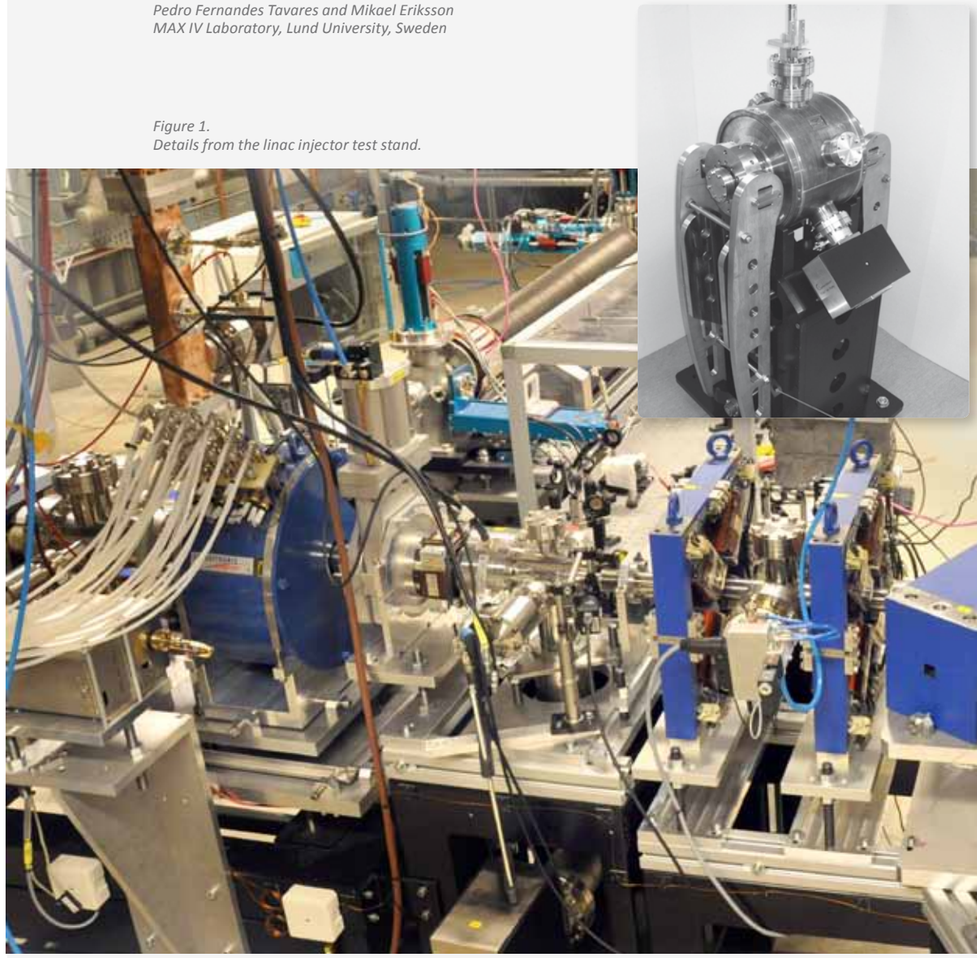

Figure 2.
Prototype harmonic cavity delivered ready for installation in the MAX III storage ring.

Figure 3.
A five-meter long prototype segment for the MAX IV linac.

These magnet blocks are particularly innovative items in the MAX IV design concept and long technical discussions with potential manufacturers were needed before a final agreement could be signed in September 2011. The contract foresees fabrication of pre-series magnets for validation of the manufacturing procedures as well as the development of dedicated magnetic characterization benches which will be used to certify that the many individual magnets sharing a common iron yoke fulfil magnet tolerance specifications.

Storage Ring Vacuum Chambers

With detailed design work and technical specifications completed a call for tender for fabrication of the so called standard chambers (which make up approximately 80% of all chambers in the 3 GeV ring) was published in December 2011. This work relied heavily on a collaboration agreement between the MAX IV Laboratory and the Spanish light source laboratory ALBA in Barcelona. The ALBA vacuum group was deeply involved in all phases of mechanical design, heat load estimates, finite element analysis and coupling impedance calculations for all vacuum chambers of both the 3 GeV and 1.5 GeV rings. The 3 GeV ring vacuum chambers have several special characteristics that single out the MAX IV design from conventional technology used at the existing light sources: the chambers feature very narrow apertures, distributed heat absorbers (the chamber itself is made in copper) are used to deal with the synchrotron radiation heat load from dipoles and insertion devices, and NEG (Non-Evaporable Getter) coating is used on a large scale (nearly 100%).

The need to NEG coat the chambers is related to the low vacuum conductance associated with the small chamber radius and the need to reduce photo-induced desorption from the intensely illuminated walls of the vacuum chamber. Given the need to implement this on a large scale and for some chambers with particularly challenging shapes, a collaboration agreement has been set up with CERN in Geneva on the development of NEG coating. The first coating tests took place in the first semester of 2012. CERN will also play a significant role in defining vacuum chamber cleaning criteria adequate for the subsequent NEG coating.

Storage Ring RF System

The RF system for both rings in MAX IV will operate at a frequency of 100 MHz and use the same technologies already developed and tested in the existing MAX-lab accelerators. A fabrication contract for all main cavities was signed in February 2011 and detailed design of a pre-series cavity was completed in the first semester of 2011. Fabrication of the pre-series started in the second semester of 2012 and delivery to MAX-lab for tests and high power conditioning took place in the first semester of 2012.

Apart from the main cavities, which provide energy to the circulating beam, restoring what was lost by emission of synchrotron radiation, so called harmonic cavities or Landau cavities will be passively operated (i.e. without a separate energy source, with excitation by the beam itself) in both MAX IV storage rings in order to lengthen the bunches, improve stability and reduce higher order mode losses. A prototype for the MAX IV Landau cavities was successfully completed and installed in the MAX III machine for tests with beam in October 2011.

Also in October, the first tests with a prototype of the low level RF system for the storage rings were successfully conducted at MAX-lab. In those tests, the accelerating cavity could be operated in a stable condition up to 10 kW input power with both frequency and amplitude loops on.

Pulsed Magnets

Detailed work on the injection dynamics for two types of injection (kicker) magnets was carried out and led to updated specifications. Dipole kickers will be used during commissioning and will also allow beam accumulation, whereas multipole kickers (recently developed, e.g. at KEK and BESSY) will provide the utmost performance allowing nearly transparent top-up injection of the rings. For fabrication of the dipole kickers a collaboration agreement is under discussion with Budker Institute of Nuclear Physics in Novosibirsk, whereas discussions are being carried out with the SOLEIL team in Paris concerning the design and construction of the multipole kickers.

1.5 GeV Ring

Detailed work on the 1.5 GeV ring started during the fall of 2011 leading to a second iteration lattice design, which will result in an updated magnet design. We expect to perform a few more iterations before the magnet specification can be fixed and a call for tender for those magnets can be published. ■

A magnet block for the 3 GeV ring as seen through a magnet block dummy.

Figure 4.
Brilliance of MAX IV compared to those of other synchrotron facilities across the world.

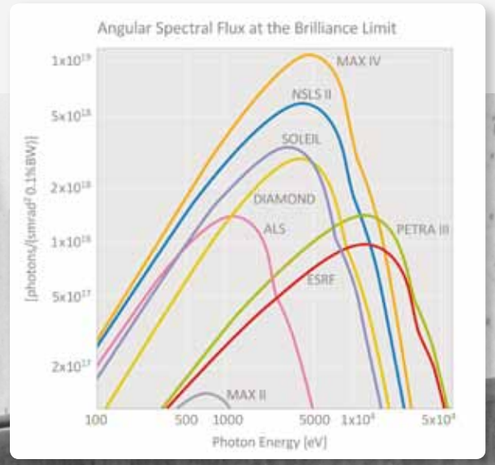

Table 1.
Comparison of the emittance of synchrotron sources from across the world.

Facility	Location	Started	Emittance, nmrad
ELETTRA	Trieste, Italy	1993	7-9.7
NANOMAX	Grenoble, France	1994	4
MAX II	Lund, Sweden	1996	8.8
BESSY II	Berlin, Germany	1998	5.2
SLS	Villigen, Switzerland	2001	5
SOLEIL	Paris, France	2007	3
DIAMOND	Oxford, UK	2007	2.74
PETRA III	Hamburg, Germany	2010	1
NSLS II	Brookhaven, USA	2015	0.6 - 1
MAX IV	Lund, Sweden	2015	0.24 – 0.36

Figure 5.
Machine Director Mikael Eriksson and a prototype magnet block awaiting characterization.

THE MAX IV BEAMLINES

Year 2011 was a very important year in the development of beamlines at MAX IV. A decision was reached about the format of the initial MAX IV beamline program and the program received funding from the Knut and Alice Wallenberg Foundation and twelve Swedish universities for the first seven beamlines at MAX IV. During the autumn of 2011, the beamline program started, a project organisation was established and time-plans were set-up.

The initial MAX IV beamline program will provide cutting-edge research infrastructures at the international forefront to the entire natural sciences community. The seven beamlines in the program are the outcome of a process with strong involvement of a range of stakeholders including Swedish research groups and technical expertise at the MAX IV Laboratory, international reviewers, and evaluation by the MAX IV Laboratory Scientific Advisory Committee (SAC), Management, and Board. During the summer and autumn of 2011, the Knut and Alice Wallenberg Foundation decided to fund the program with 400 MSEK and twelve Swedish universities provided co-funding of 162 MSEK. Efforts at obtaining funding for additional beamlines are currently on-going.

The following seven beamlines are included in the program (see also Figure 1 and Table 1):

- **FemtoMAX**: A beamline situated on the extension of the linac to facilitate studies of the structure and dynamics of materials with X-ray pulses of 100 fs duration.
- **NanoMAX:** A hard X-ray beamline for micro- and nanobeams.
- **XAS:** A beamline for *in-situ* hard X-ray spectroscopy.
- **BioMAX:** A multipurpose high throughput beamline for macromolecular crystallography.
- **VERITAS:** A beamline for soft X-ray Resonant Inelastic X-ray Scattering (RIXS).
- **HIPPIE:** A state-of-the-art beamline for high pressure X-ray photoelectron spectroscopy (HP-XPS), high pressure X-ray absorption spectroscopy (HP-XAS) as well as XPS and XAS in ultrahigh vacuum.
- **ARPES:** A beamline for angle resolved photo electron spectroscopy (ARPES).

Researchers from Swedish universities were closely involved in the definition and development of the beamline proposals and continue to be so also during the construction phase via participation in the workgroups defined for each beamline. The strong involvement from Swedish universities provides access to experience and knowledge not available at the MAX IV Laboratory and additionally increases the coupling to the Swedish research community. An open access policy, with peer review of proposals and free-of-charge use, will ensure that the beamlines are available to the entire community and for the best experiments.

In September 2011, the beamline program started with a workshop for the beamline-project workgroups and key MAX IV personnel. During the autumn of 2011, the beamline construction organisation was established and documented, time-plans were created and partially resource loaded, and financial reporting schemes were discussed and implemented within the beamline construction organisation.

The technical issues of the beamlines have been further developed and described in design reports for all beamlines. Evaluation of these reports will be completed during October 2012. As of early autumn 2012, the construction of the beamlines is on time and budget. First operation is expected late 2015 or early 2016. Further and updated information on the beamlines can be found at https://www.maxlab.lu.se/BPO.

Late 2011, a Cooperation Agreement in the field of synchrotron light research was signed between SOLEIL and the Swedish Research Council. This agreement laid the foundations for collaborations between SOLEIL and the MAX IV Laboratory in several areas of high importance for the beamline development at the MAX IV Laboratory. For instance, projects of immediate importance for the Initial MAX IV beamline program were established within general beamline and sample environment development, within research and development on nano-beamlines, and within time-resolved methods.

The seven beamlines within the Initial MAX IV beamline program only exploit approximately 25% of the full capacity of the MAX IV facility. They represent a reduction of the present capacity at MAX-lab with its current 20 experimental stations and also address only partially the needs of the synchrotron community with some key research methods and areas lacking. Further beamlines which address these issues as well as make use of the possibilities presented by the unique cutting-edge emittance and coherence

Figure 1.
MAX IV and the location of the seven beamlines in the Initial MAX IV Beamline Program (see also Table 1).

of the MAX IV radiation are described in a Strategic Plan 2012-2020 submitted to the Research Council May 2, 2012. The Strategic Plan also include suggestions for transfer of existing beamline equipment to the 1.5 GeV ring as well as several beamlines that have been suggested for funding by neighbouring countries. Developing the beamlines in the Strategic Plan into a program that provides the best possible support for the research community around the MAX IV facility, as well as obtaining funding for such a program, is a major task for the future of the MAX IV Laboratory. ■

Table 1.
Beamlines constructed in the Initial MAX IV Beamline Program

Name	Number	Energy range	Facility	Methods	Main area(s) served
FemtoMAX	1	1.8 - 30 keV	linac	Femto-second X-ray scattering, EXAFS and Spectroscopy	Physics, Chemistry, Accelerator development
NANOMAX	2	5 - 15 keV (optimal)	3 GeV ring	Scanning X-ray Microscopy, X-ray Fluorescence and scatte-ring techniques such as XRD, SAXS/ WAXS, Coherent XRD	Nano-science, Materials Science
XAS	3	4 - 40 keV	3 GeV ring	(*in-situ*) XAS	Materials & Environmental Science, Energy research, Cultural heritage
BioMAX	4	5 - 25 keV	3 GeV ring	Diffraction	Life-science
VERITAS	5	275 - 2000 eV	3 GeV ring	RIXS (Resonant Inelastic X-ray Scattering)	Physics, Chemistry, Materials Science
HIPPIE	6	260 - 2000 eV	3 GeV ring	High Pressure XPS (X-ray Photoelectron Spectroscopy)	Chemistry, Catalysis, Corrosion, Materials Science, Physics
ARPES	7	10 - 1000 eV	1.5 GeV ring	Angle resolved photo electron spectroscopy	Physics, Nano-science, Materials Science

SCIENTIFIC HIGHLIGHTS

NEW TOOLS FOR OLD MOLECULES

What did the dinosaurs really look like? Were their flesh and bones different from ours? Studies of proteins and pigments in 50-70 million year old fossils show that the similarities between prehistoric and modern animals are greater than we knew before.

Figure 1. Picture of a fossilized mosasaur skull.

For a long time, studies of ancient life relied on fossilized hard parts, such as bones and shells, to provide evidence on extinct creatures and how they lived. That is, virtually all original organic components of the organisms were presumed lost or altered in such a way that they were unrecognizable, normally within well under a million years. It was therefore assumed that what remains today of the organic content in fossils on a molecular level have nothing to do with the animal when it was alive.

However, during the last decade a different view on the prehistoric world has begun to emerge. An increasing number of scientists now believe that biomolecules, under certain circumstances, can be preserved in fossils many millions of years old. These discoveries are provocative and potentially revolutionary; biomolecules that originate from multimillion-year-old animals can still be detected and hence analysed. In 2010, Science Magazine coined it one of ten insights that have changed science since the dawn of the new millennium [1, 2].

To support the hypothesis that original biomolecules can be preserved over deep time we obtained hard-core molecular spectroscopic data from two entirely different types of samples; bony tissues from a 70 million-year-old giant marine lizard (a mosasaur) and a 54 million-year-old fish eye. The IR microscope at beamline D7 at MAX III was used for these studies and a number of additional analytical techniques were applied to corroborate our results.

Collagen is a naturally occurring protein in animals where it constitutes up to 35% of the whole-body protein content. It is found in the form of elongated fibrils and mostly occur in tissues, such as tendons, ligaments, as well as in the skin. It is also the main organic component of bone. When analysing demineralized bone samples from a 70 million-year-old mosasaur we were able to show spectroscopic data from 150 × 150 µm fibrous bony tissues. Our data showed that the bony tissues exhibit a spectroscopic signature consistent with type I collagen [3]; that is, the spectroscopic data were recorded at sites where fibrous tissues with a morphology consistent with collagen were located. Preservation of type I collagen has previously been demonstrated, e.g. in a bone of the theropod dinosaur Tyrannosaurus rex [4]; however, no clear connection between structure/morphology and spectroscopic data was made in that study.

Similarly, the coloring of extinct animals, including a small Jurassic dinosaur, has recently been inferred based on a reinterpretation of microstructures, about 2 µm long, in feathered fossils. These structures were previously believed to be remains of bacterial biofilms, but are now interpreted as colour-bearing organelles, or melanosomes [5, 6]. However, this latter interpretation was based only on morphology, without any molecular spectroscopy, leaving alternative interpretations liable. By analysing a 54 million-year-old bony fish eye we have demonstrated that not only is the characteristic morphology of melanosomes preserved, but they also contain high concentrations of the pigment melanin [7]. Indeed, the spectroscopic signature of melanin in the fossil was indistinguishable from that of a modern reference sample obtained from ink sacs of the squid Sepia officinalis. ■

J. Lindgren[c], P. Uvdal[a, b], A. Engdahl[b]

a. Chemical Physics, Department of Chemistry, Lund University, Sweden
b. MAX IV Laboratory, Lund University, Sweden
c. Department of Geology, Lund University, Sweden

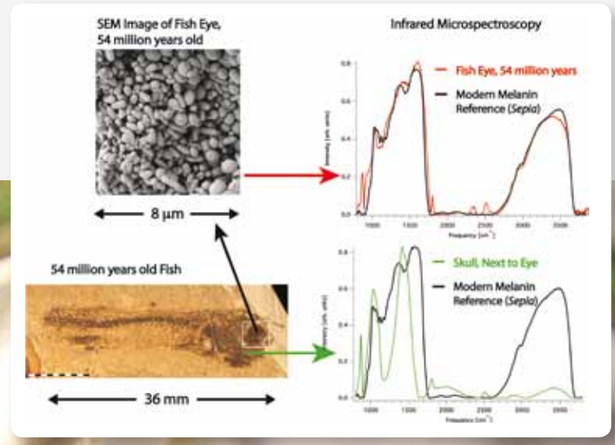

Figure 2.
Lower left: Picture of a 54 million year old fish fossil from the Fur formation in Denmark. Top left: SEM image of the eye showing melanosome-like structures. Right: IR spectra of the fossil eye (top) and skull (bottom) compared to the spectrum of a melanin reference sample.

Figure 3.
ToF-SIMS spectra of melanin and melanosomes from a 54 million year old fish fossil. The agreement between the two spectra shows that the melonosome-like structures in the eye (insert) contain large amounts of melanin. Data collected at SP Technical Research Inst. of Sweden, in Borås by P. Sjövall.

References:
1. The news staff, Science 330, 1612 (2010).
2. A. Gibbons, Science 330, 1616 (2010).
3. J. Lindgren, P. Uvdal, A. Engdahl, A. H. Lee, C. Alwmark, K.-E. Bergquist, E. Nilsson, P. Ekström, M. Rasmussen, D. A. Douglas, M. J. Polcyn, L. L. Jacobs, PLoS ONE 6, e19445 (2011).
4. M. H. Schweitzer, Z. Suo, R. Avci, J. M. Asara, M. A. Allen, F. Teran Arce, J. R. Horner, Science 316, 277 (2007).
5. Q. Li, K.-Q. Gao, J. Vinther, M. D. Shawkey, J. A. Clarke, L. D'Alba, Q. Meng, D. E. G. Briggs, R. O. Prum, Science 327, 1369 (2010).
6. F. Zhang, S. L. Kearns, P. J. Orr, M. J. Benton, Z. Zhou, D. Johnson, X. Xu, X. Wang, Nature 463, 1075 (2010).
7. J. Lindgren, P. Uvdal, P. Sjövall, , D. E. Nilsson, A. Engdahl, B. Pagh Schultz, V. Thiel, Nature Com. DOI 10.1038/ncomms1819 (2012).

AMBIENT PRESSURE XPS AT MAX II

J. Schnadt[a], J. Knudsen[a], N. Johansson[a], A. Pietzsch[b], F. Hennies[b], M. Andersson[b], G. Öhrwall [b], N. Mårtensson[c], H. Siegbahn[c], and J. N. Andersen[a,b]

a. Division of Synchrotron Radiation Research, Lund University, Sweden
b. MAX IV Laboratory, Lund University, Sweden
c. Department of Physics and Astronomy, Uppsala University, Sweden

A new method (ambient pressure X-ray photoelectron spectroscopy) has recently been implemented at the MAX II ring. During measurements the samples can remain in a more natural state when examined, which implies that researchers can look into how a sample is affected by a gas atmosphere. The new instrument opens up for materials research in areas like catalysis and oxidation.

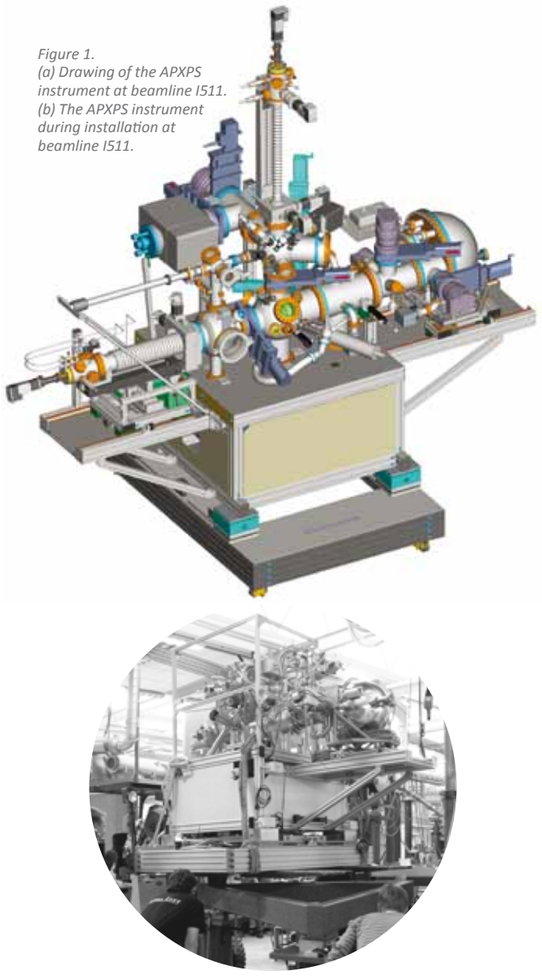

Figure 1.
(a) Drawing of the APXPS instrument at beamline I511.
(b) The APXPS instrument during installation at beamline I511.

Since September 2011 beamline I511 on the MAX II ring accommodates a new instrument for ambient pressure X-ray photoelectron spectroscopy (APXPS), a technique which allows X-ray photoelectron spectroscopy (XPS) measurements at ambient pressures of some mbar [1]. At present, the maximum pressure of our instrument is at around 2 to 3 mbar, which should increase by an order of magnitude after the beamline has been rebuilt to become the SPECIES beamline in 2013. Here, we briefly present the new instrument [2] and selected user results obtained during the past year.

Figure 1a shows a drawing of the instrument. It makes use of a PHOIBOS 150 NAP SPECS analyser in combination with a high pressure cell (Figure 5). The cell was developed by SPECS based on our idea of enabling dual ultrahigh vacuum (UHV) and ambient pressure usage by restricting the ambient pressure environment to the HP cell which can be docked to the analyzer. In UHV mode the cell is retracted from the analysis chamber and valved off, and proper UHV conditions are achieved swiftly.

Figure 2 shows data obtained on a stainless steel surface. The goal was to study the oxidation of the surface as a function of sample temperature and oxygen pressure and in particular the role of oxygen adsorption induced segregation of alloy constituents during oxidation.

The XP spectra obtained in UHV are distinctly different from those measured at 0.04 to 0.3 mbar ambient oxygen pressure. Also the temperature plays an important role: heating to 423 K leads to a strong preferential segregation of Fe to the surface and concomitant oxidation to Fe^{2+} and Fe^{3+}. This is accompanied by a reduction of the Cr^{3+} surface concentration.

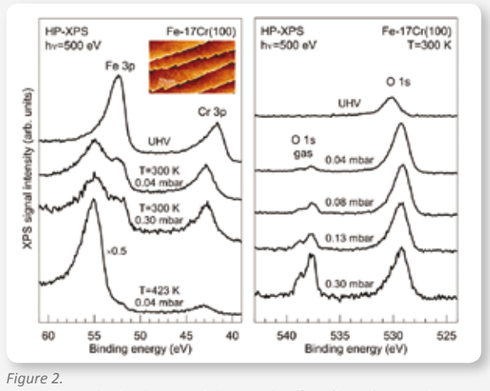

Figure 2.
XPS spectra obtained on a stainless steel surface (insert) at varying oxygen pressures.

Figure 3 shows XPS data from a Pd(111) surface that is exposed to 0.5 mbar methanol. A graphitic phase is formed, which blocks the surface sites from further reaction. Depth probing with different photon energies shows that the graphitic phase is localized on the surface. Once oxygen gas is introduced the graphitic phase is partially removed at 130 °C and fully at 330 °C.

Figure 4 shows an example of simultaneous recording of mass spectrometer reactivity data (upper row) and XP spectra (lower row) when CO is oxidized over a Ir(111) surface. At low temperatures the O 1s spectra contain peaks for oxygen gas and a signal characteristic of adsorbed CO. Upon heating to 500 K the XP spectra drastically change their appearance: the CO surface peak is partly replaced by an oxygen surface peak and, in addition, a CO_2 gas phase signal is observed. At the same temperature the mass spectrometer data shows the ignition of the oxidation reaction. Thus, CO poisons the surface at low temperatures, while a coexisting structure of adsorbed CO and oxygen is present on the surface in the active phase.

The results presented above exemplify the capabilities of the new instrument for APXPS. Our conclusion is that APXPS is a very valuable tool for the study of oxidation, catalytic reactions, and in general the influence of an ambient gas atmosphere on the structure of a sample. In particular, APXPS allows the *in-situ* study of phases which require ambient pressures for formation and existence.

We would like to thank Mika Hirsimäki and Mika Valden (Tampere University of Technology) and Christian Weilach (Technical University of Vienna) for providing us with results from their beamtimes. The Knut and Alice Wallenberg Foundation is gratefully acknowledged for funding the APXPS instrument. ■

References:
1. D. F. Ogletree, H. Bluhm, G. Lebedev, C. S. Fadley, Z. Hussain, M. Salmeron, Rev. Sci. Instrum. 73, 3872 (2002); H. Bluhm, M. Hävecker, A. Knop-Gericke, E. Kleimenov, R. Schlögl, D. Teschner, V. I. Bukhtiyarov, D. F. Ogletree, M. Salmeron, J. Phys. Chem. B 108, 14340 (2004); M. Salmeron, R. Schlögl, Surf. Sci. Rep. 63, 169 (2008).
2. J. Schnadt, J. Knudsen, J. N. Andersen, H. Siegbahn, A. Pietzsch, F. Hennies, N. Johansson, N. Mårtensson, G. Öhrwall, S. Bahr, S. Mähl, O. Schaff, J. Synchrotron Rad., submitted (2012).

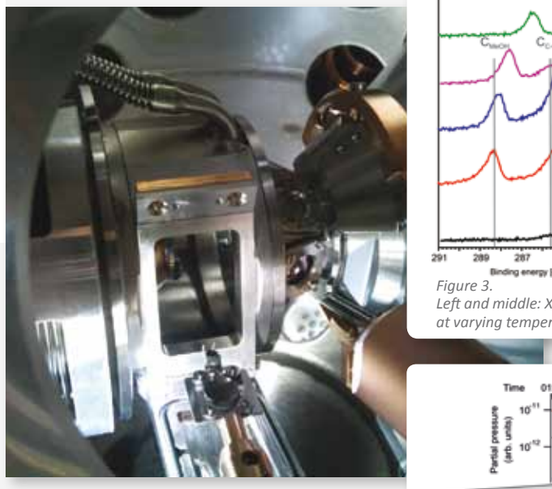

Figure 5.
The high pressure cell in the APXPS instrument.

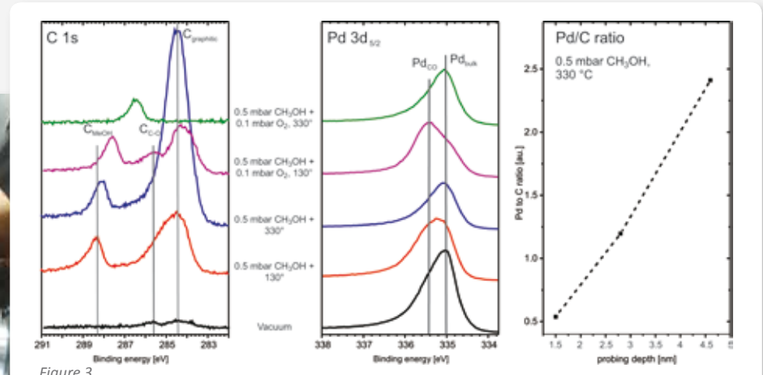

Figure 3.
Left and middle: XPS data obtained on a Pd(111) surface exposed to a 0.5 mbar methanol pressure at varying temperatures. Right: Probing depth dependency of the Pd/C ratio.

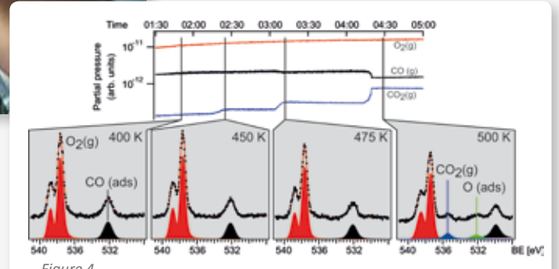

Figure 4.
XP spectra (lower row) and mass spectrometer data (upper row) recorded simultaneously on a Ir(111) surface while increasing the temperature.

XAS APPLIED ON ENVIRONMENTAL ISSUES

P. Persson[a] and I. Persson[b]

a. Department of Chemistry, Umeå University, Sweden
b. Department of Chemistry, BioCenter, SLU, Uppsala, Sweden

With in-depth knowledge about the chemistry of soils and natural waters, we can better understand some of the Earth's environmental challenges. Recent research at MAX-lab shows how iron interacts with natural organic material in soil, and how it affects nutrients and contaminants. The fascinating surface films in lakes and pools have also been examined and their interesting role in the biological-geological-chemical systems is now being unfolded.

The awareness of the importance to understand and model Earth surface systems at the molecular level and under *in-situ* conditions has stimulated much recent research [1]. Here modern spectroscopic methods, and in particular synchrotron-based techniques, play a unique and central role.

Many environmental processes have complex mechanisms that must be understood at a fundamental level in order to develop models for predicting the behavior of nutrients and contaminants in aquatic systems or soils. Spectroscopic methods, e.g. synchrotron-based X-ray absorption spectroscopy (XAS), are well suited to provide molecular-level information about these processes, the reaction products resulting from them, and reaction intermediates that control overall reaction rates. Such methods are also needed to understand the complex interactions among microorganisms, natural solids, and contaminant ions and molecules in terrestrial and aquatic environments. Thus techniques are needed for *in-situ* speciation studies, which offer both high sensitivity (due to the often low contaminant and nutrient concentrations) and high spatial resolution.

Continued on next page...

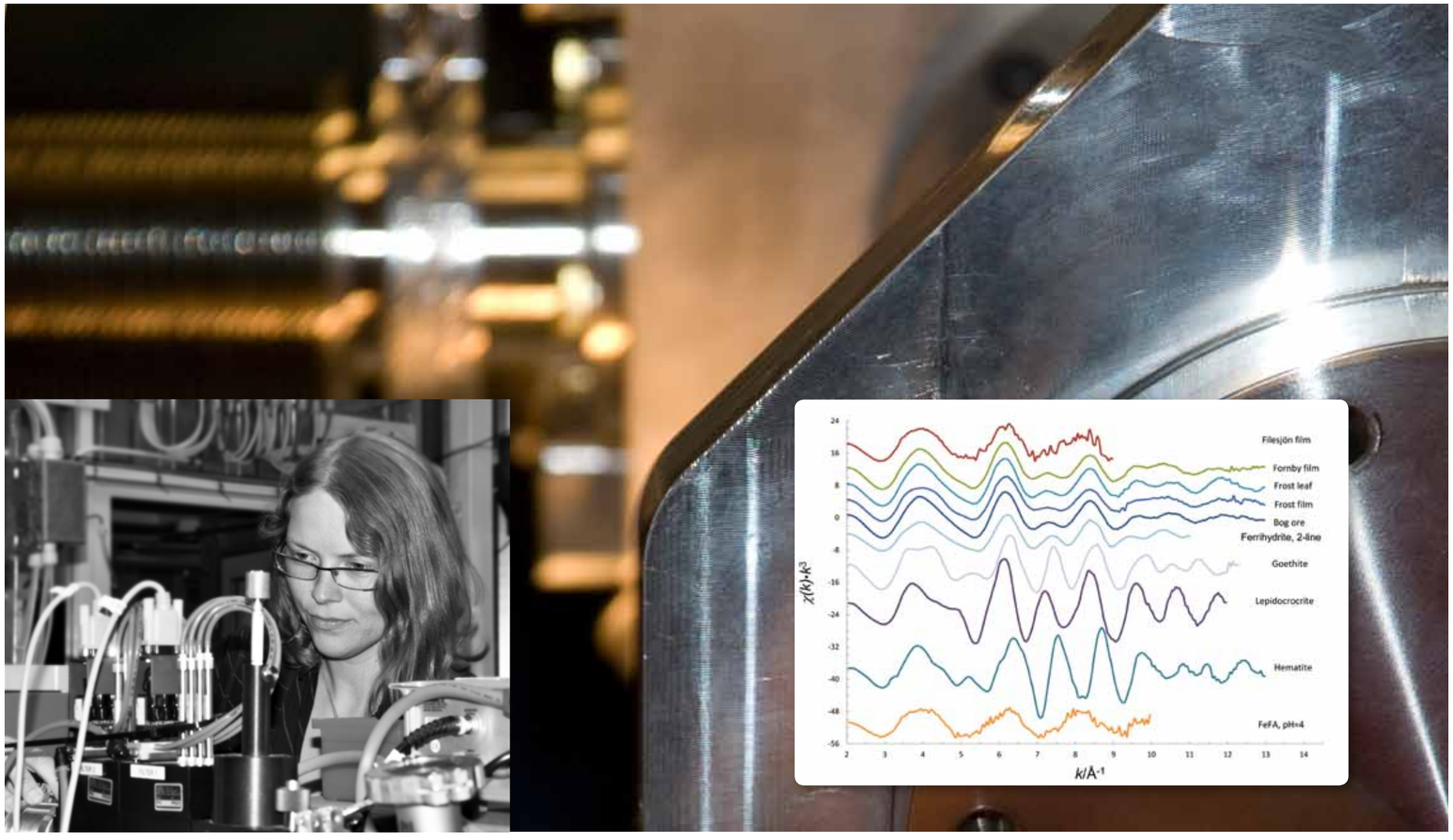

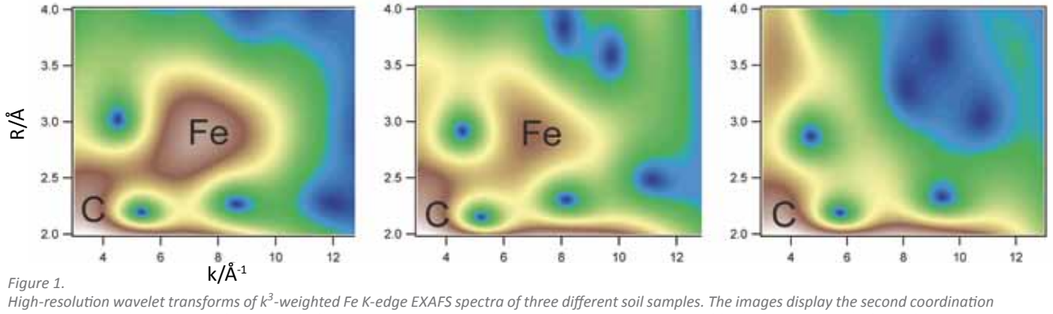

Figure 1.
High-resolution wavelet transforms of k^3-weighted Fe K-edge EXAFS spectra of three different soil samples. The images display the second coordination shell and show an increasing relative concentration of mononuclear organic Fe(III)-NOM complexes from left to right, which is indicated by the decreasing intensity of the Fe-Fe scattering contribution. Data are plotted as a function of k (Å^{-1}) on the x-axis and R (Å) on the y-axis.

Figure 2.
Stacked, normalized k^3-weighted EXAFS spectra for iron in natural films and precipitates. The spectra for synthetic 2-line ferrihydrite, goethite, lepidocrocrite, hematite and an iron(III)-fulvic acid complex at pH 4.0.

Figure 3.
Floating, iron bearing film from a well at Fornby in the middle part of Sweden.

One example where synchrotron-based techniques have provided a wealth of new and fundamental information is the environmentally significant interactions between Natural Organic Matter (NOM) and iron and its oxides. These interactions tightly couple the biogeochemical cycles of carbon and iron, and thus have several far-reaching implications; e.g. for nutrient availability and carbon turnover in soils and natural waters, and therefore also for climate change. By means of synchrotron-based XAS we have shown that NOM stabilizes mononuclear Fe(III) chelate complexes via strong interactions with carboxyl groups of the organic material [2-4]. NOM also favor the formation of very small iron hydroxide nanoparticles. Both these species are readily identified by quantitative non-linear least squares fitting of EXAFS spectra or qualitatively from wavelet transforms of EXAFS spectra as shown in Figure 1.

The possibility to determine the relative concentration of organic Fe(III)-NOM complexes and iron hydroxides is of great biogeochemical significance as the distribution will affect the reactivity of iron towards nutrients and contaminants as well as the stability of NOM. The influence of iron and iron-containing nanoparticles on NOM is, however, complex and will not only have a stabilizing effect. For example, we have shown in a recent study that degradation of NOM by ectomycorrhizal (EM) fungi is driven by the iron redox and Fenton chemistry [5]. Thus, the reactivity of iron species is linked to the turnover of carbon in soils.

The application of *in-situ* spectroscopic probes in environmental science, and of the importance of obtaining molecular information on chemical speciation and its link to biological activity and risk assessment is the behavior of the well-known herbicide glyphosate (i.e. the active component in RoundUp) in soils. In a series of studies we have determined the molecular forms of glyphosate under various conditions [6-8], and we have also shown that interaction with biota is very much determined by the specific form [9]. Some forms, such as the free glyphosate molecule in aqueous solution, are mildly toxic while others, for example glyphosate adsorbed to iron oxides via the phosphonate group, are non-toxic and may be used as carbon sources by soil microorganisms. Thus, in order to make a proper risk assessment of glyphosate, we need to understand at a molecular level how biota interacts with this anthropogenic herbicide.

The surface of undisturbed water in lakes and pools has sometimes an oily gleam due to the presence of a very thin film, Figure 3. These films are fragile and break easily down and become suspended into the water upon disturbance from e.g. wind and rain. To date, the knowledge about the formation and composition of these iron-bearing films is scarce. We have investigated the form of iron in floating iron-rich films from a wide range of environments, including a pond and a brook, as well as seep water pools of a groundwater discharge area [10]. Sampling sites were located in southern (pond, brook) and central (seep pools) Sweden.

Synchrotron-based X-ray absorption spectroscopy (EXAFS and XANES) performed at beamline I811, MAX-lab, Lund University, allowed identification of the iron precipitates present in the films, without any pretreatment, Figure 2. The EXAFS data showed that the iron containing phase formed in the floating films varied in composition between the sites investigated. In the two ground water discharge areas, characterized by out-flowing iron(II) rich ground water being high in pH and low in dissolved natural matter (NOM), the films were completely dominated by ferrihydrite. In contrast, surface films sampled from the brook and the pond consisted of a mixture of iron(III)-NOM complexes and ferrihydrite. These waters were oxic and contained higher concentration of NOM than the seep water pools in the ground water discharge areas. Elemental composition of one film (seep water), suggested that films contained about one third of organic matter. Ferrihydrite is probably present as small particles with humic material sorbed onto surfaces or included in the particles, making the particles sufficiently hydrophobic to not settle without physical disturbance. The composition of bog ore is approximately the same as observed in these surface films from seep water, and that bog ore has formed through accumulation of these surface films. More studies are warranted in order to understand the mechanism of the formation of these fascinating films and their biogeochemical role. ■

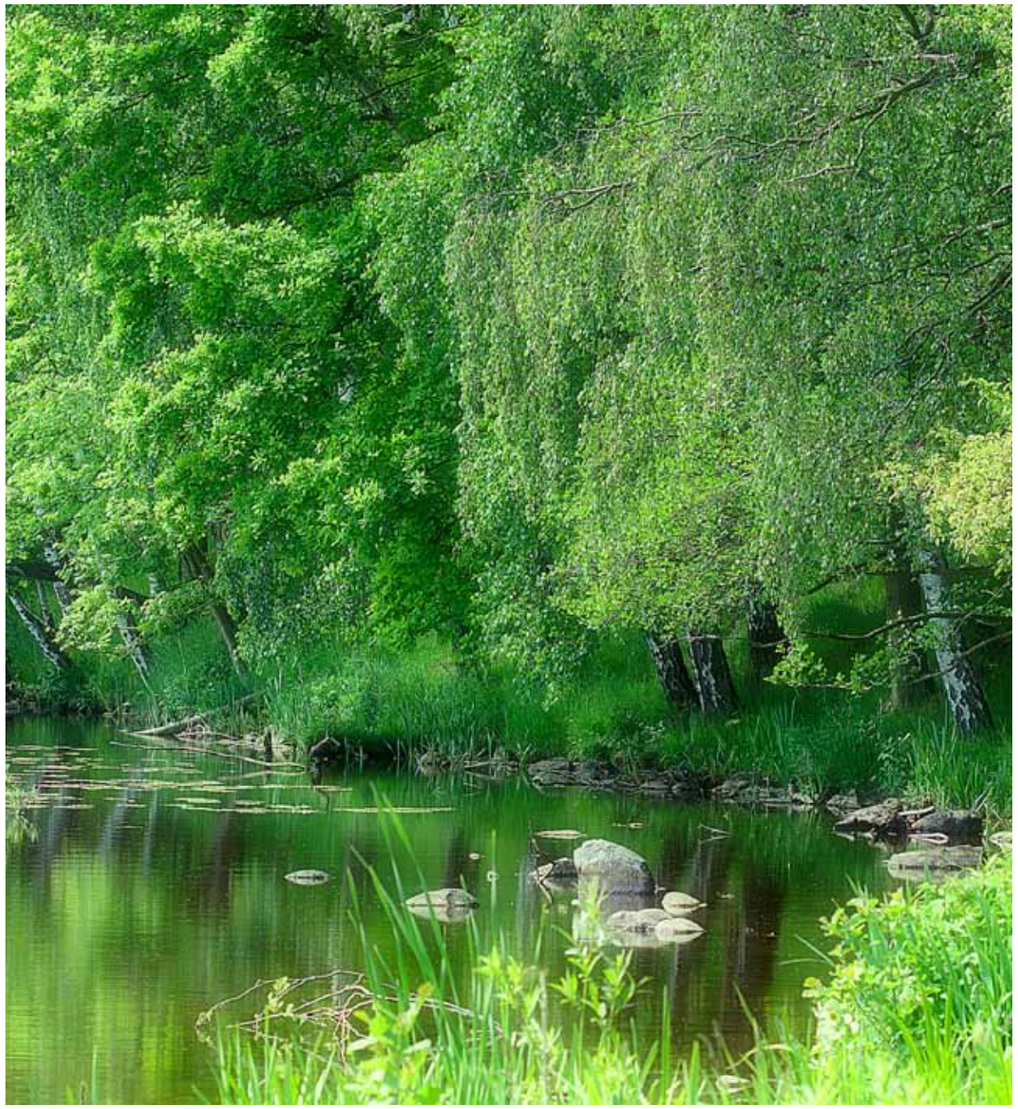

References:

1. *MW.I. Schmidt, M. S. Torn, S. Abiven, T. Dittmar, G. Guggenberger, I. A. Janssens, M. Kleber, I. Kögel-Knabner, J. Lehmann, D. A. C. Manning, P. Nannipieri, D. P. Rasse, S. Weiner, S. E. Trumbore, Nature 478, 49 (2011).*
2. *T. Karlsson, P. Persson, U. Skyllberg, C-M Mörth, R. Giesler, Environ. Sci. Technol. 42, 5449 (2008).*
3. *T. Karlsson, P. Persson, Geochim. Cosmochim. Acta 74, 30 (2010).*
4. *T. Karlsson, P. Persson, Chem. Geol., in press.*
5. *F. Rineau, D. Roth, F. Shah, M. Smits, T. Johansson, B. Canbäck, P. Bjarke Olsen, P. Persson, M. Nedergaard Grell, E. Lindquist, I. V. Grigoriev, L. Lange, A. Tunlid, Environ. Microbiol. Rep. 14, 1477 (2012).*
6. *J. Sheals, P. Persson, B. Hedman, Inorg. Chem. 40, 4302 (2001).*
7. *J. Sheals, S. Sjöberg, P. Persson, Environ. Sci. Technol. 36, 3090 (2002).*
8. *J. Sheals, M. Granström, S. Sjöberg, P. Persson, J. Colloid Interf. Sci. 262, 38 (2003).*
9. *Y. Schnürer, P. Persson, M. Nilsson, A. Nordgren, R. Giesler, Environ. Sci. Technol. 40, 4145 (2006).*
10. *D. Berggren Kleja, J. W. J. van Schaik, I. Persson, J. P. Gustafsson, Chem. Geol. 326-327, 19 (2012).*

DETECTING PHOTONS

Bent Schröder
MAX IV Laboratory, Lund University, Sweden

Detection of photons, the smallest “energy packet” in the electromagnetic field, has for a long time provided valuable information with high precision in nuclear physics experiments. At MAX-lab, the tagged photon facility is currently used for the development of photon detectors and for precision photonuclear experiments.

More than 50 % of the experiments at the tagged photon facility at MAX I are connected with photon detection and photon detectors. Two examples of such experiments are presented below; one concerning the properties of a relatively new scintillator (PWO) and the other describing the use of the well-known NaI(Tl) detector to register scattered photons from a deuterium target.

Response of the PWO crystals to photons below 100 MeV
An Uppsala – Stockholm – Lund Collaboration

The future Facility for Antiproton and Ion Research (FAIR) at GSI in Darmstadt will provide opportunities to study a wide range of topics in physics. One of the major experiments at FAIR is PANDA at the high energy storage ring HESR, where antiprotons in the energy range 1– 15 GeV will be used to study the structure and interaction of hadrons.

The PANDA detector with a total length of ~ 14 m (Figure 1) will have excellent particle identification, energy resolution and spatial resolution. Anti-protons enter the detector from the left and interact with protons or nuclei in the center of the cylindrical detector part. One very essential part is the detection of photons in the Electromagnetic Calorimeter (EM). Swedish groups from Uppsala, Stockholm and Lund are deeply involved in the design and construction of the forward part of the EM, which consists of 3600 crystals with dimensions 2 x 2 x 20 cm^3. The EM will be required to detect photons down to about 10 MeV. The tagged photon facility at MAX-lab is ideally suited to study the response of the PWO crystals.

The response of a matrix of 5 x 5 crystals to low-energy photons was studied at MAX-lab. The crystals were kept at -25 °C in a climate chamber. The relative energy resolution σ/E is shown as a function of photon energy E for different energy thresholds in Figure 3. The best resolution is obtained for a threshold of 0.5 MeV.

Deuteron Compton Scattering
A Compton@MAX-lab Collaboration

The external electric and magnetic fields **E** and **B** of photons will induce electric and magnetic dipole moments, **p** and **m**, in a system such as a nucleon. The dipole moments are proportional to the fields, $\mathbf{p} = \alpha \mathbf{E}$ and $\mathbf{m} = \beta \mathbf{B}$. The factors α and β are the electric and magnetic polarizabilities of the system. Like mass, charge and intrinsic dipole moments, polarizabilities are fundamental characteristics of a system. α is related to the stiffness of the system, for the proton $\alpha \approx 12 \times 10^{-4}$ fm^3 which may be compared to the volume $V \approx 1$ fm^3, thus the proton is stiff. The polarizabilities may be determined experimentally from studies of elastic photon scattering. Several experiments, with hydrogen targets, have studied the proton polarizabilities, thus α_p and β_p are accurately known. Since there are no free neutron targets, one needs nuclear targets, the simplest being a deuterium target.

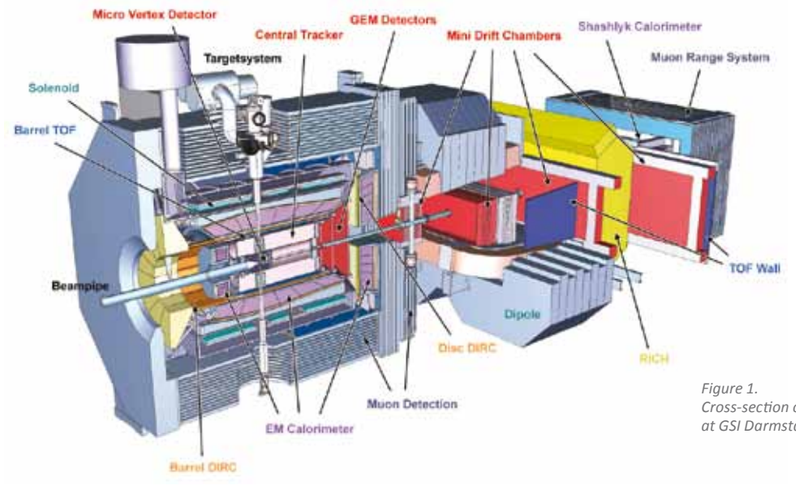

Figure 1.
Cross-section of the PANDA detector at GSI Darmstadt.

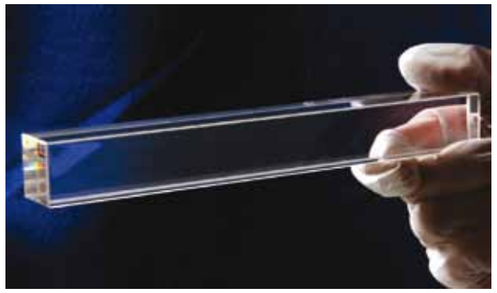

Figure 2.
A PWO crystal.

The differential cross sections dσ/dΩ for elastic photon scattering from deuterium at photon energies 55, 66 and 94 MeV, respectively are shown as a function of scattering angle θ in Figure 4. The experimental data were obtained at Illinois (open circles), Lund (filled circles) and Saskatoon (open squares). The scattering cross section shows the following angle dependence

$$d\sigma/d\Omega \sim (\alpha + \beta) \times (1 + \cos\theta_\gamma)^2 + (\alpha - \beta) \times (1 - \cos\theta_\gamma)^2$$

The different angular dependence can be used to extract both α and β. For deuterium the isospin averaged polarizabilities are obtained, to deduce the neutron polarizabilities, the proton values have to be subtracted.

The curves show theoretical predictions for varying values of α_N and β_N. For the 55 and 66 MeV data, $\alpha_N = 11.9$ and $\beta_N = 5.5$ (in units of 10^{-4} fm^3) was obtained. The relative scarcity of data for the neutron led the Compton@MAX-lab Collaboration to investigate elastic photon scattering from deuterium at the tagged photon facility at MAX-lab. Three large NaI(Tl) spectrometers were collected with energy resolutions around 2 % which is required as deuterium break up at 2.2 MeV. The CATS spectrometer is shown inside the lead shield in Figure 5.

Deuterium Compton scattering has so far been investigated in the energy region 65 to 115 MeV with NaI spectrometers at scattering angles 60°, 120° and 150°. The first results were presented in the PhD thesis of Luke Myers, University of Illinios. The final analysis of this data set is expected soon. In a second PhD project, Khayrullo Shoniyozou, University of Kentucky, is analyzing an independent data set at photon energies near 100 MeV at three different scattering angles. We plan to extend the studies of deuterium Compton scattering to the energy range 145 - 165 MeV. Within the Compton@MAX-lab Collaboration there is a fruitful interaction between theory and experiment which will facilitate the interpretation of the experimental results. ■

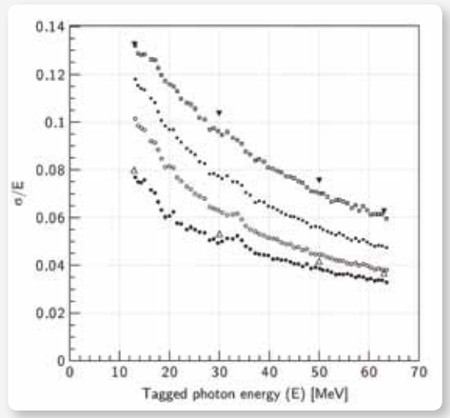

Figure 3.
Energy resolution σ/E vs photon energy E for different energy thresholds. Results for different thresholds are compared: 0.5 MeV (filled circles), 1.0 MeV (empty circles), 1.8 MeV (filled squares) and 3.0 MeV (empty squares). For comparison, results obtained from simulated data are shown for a 0.5 MeV threshold (empty triangles) and for a 3.0 MeV threshold (filled triangles).

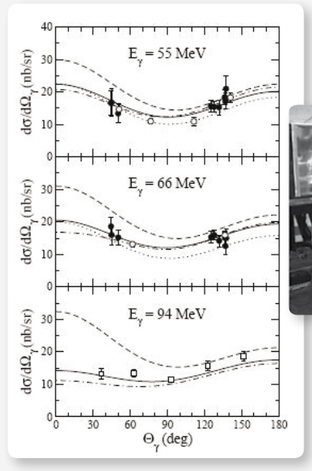

Figure 4.
Differential cross sections dσ/dΩ for elastic photon scattering from deuterium at photon energies 55, 66 and 94 MeV as a function of scattering angle θ_γ.

Figure 5
The CATS spectrometer at MAX I.

References:
K. Marcks von Würtemberg, L. Gerén, O. Lundberg, P. -E. Tegnér, K. Fransson, S. Grape, T. Johansson, E. Thomé, M. Wolke, J. Brudvik, K. Fissum, K. Hansen, L. Isaksson, M. Lundin, B. Schröder, Nucl. Instr. Meth.in Phys. Res. A 679, 36 (2012).

HIGHLIGHTS FROM THE I911 MX BEAMLINES

A. Labrador[a], J. Unge[a], R. Appio[a], F. Fredslund[a], T. Ursby[a], M. Thunnissen[a,b]
a. MAX IV Laboratory, Lund University, Lund, Sweden
b. Department of Biochemistry and Structural Biology, Lund University, Sweden

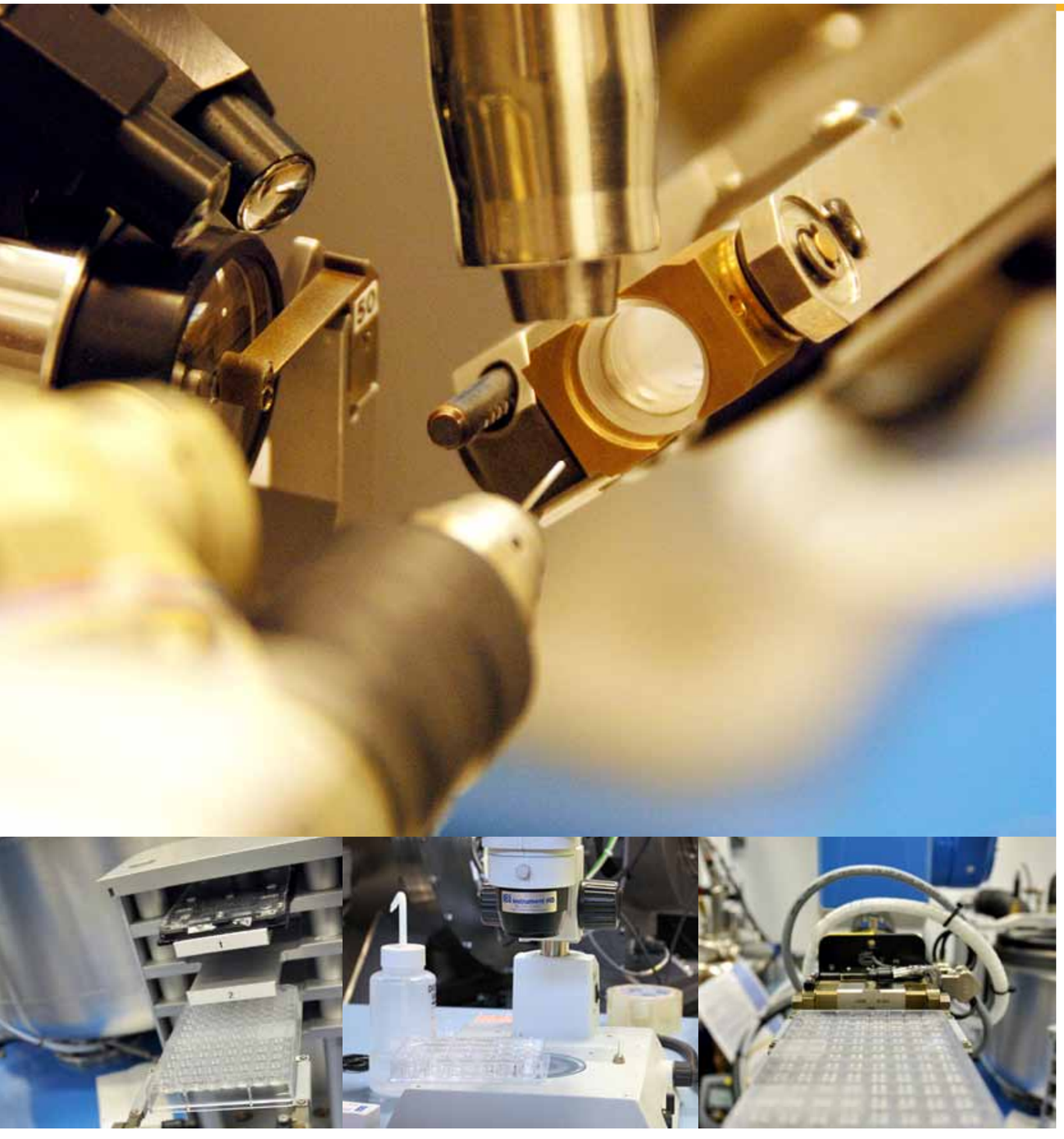

Two exciting projects at the Cassiopeia beamline show the importance of synchrotron radiation in the determination of protein structures. One is investigating copper transport across the cell membrane acquiring knowledge that can lead to new therapies for diseases caused by genetic defects. It can also serve as a base for the development of a new class of antibiotics. Another project examined the structure of a human protein, glypican-1, which provides important information about diseases affecting the growth of the human body.

Structural investigations of proteins are a fundamental part of modern life-science research. Since proteins are involved in virtually all processes that make life, they are essential for all organisms.

The many different processes that proteins are involved in stretch from the way that replication (DNA copying) occurs, through the way that cells develop and specialise to the maintenance and defense of our bodies, or the way we receive signals from the outside world (vision, touch, smell…).

The functions of proteins are affected in many different diseases, and infectious agents such as bacteria or viruses use proteins to help them invade our bodies. Most of our modern-day medicines bind to proteins, whether from our own bodies or from these “foreign invaders”.

Apart from the many different functions and tasks that proteins perform, they also have many shapes and sizes, from small enzymes that function alone to proteins that form huge complexes with other important biological molecules such as RNA or DNA. They can be soluble – floating freely in or between cells – or tightly embedded in cell membranes.

Because of this wealth of variety in the proteins themselves and the processes they are involved in, it is important to study these important molecules in depth. X-ray crystallography is one of the most powerful techniques to study proteins and their complexes. The proteins are crystallised and subsequent exposure by X-rays can reveal minute details of the structure of these molecules. These structural details make it possible to study the function of the proteins, how they interact with their partners or how they catalyse reactions. Synchrotrons play an essential role in the way that data is collected for these studies. They provide a highly intense X-ray beam that can be used to study even extremely small samples.

Two recent examples of structures revealed by using data from beamline I911 at MAX-lab are prime examples of both the diversity of proteins and also how the structural details are essential for functional studies that lead to better understanding of the specific roles these proteins play.

The first example is the structure of the copper-transporting PIB-type ATPase (Cu^+-ATPase), a membrane protein, investigated by the group of Prof. Poul Nissen in Aarhus [1]. This particular protein is important for maintaining the correct amount of copper within cells. Copper is needed for many different processes (e.g. respiration or translation) and it is thus an essential metal that is required by living cells. However, too much copper is very toxic; thus the levels of copper within cells need to be tightly regulated and excess copper should be removed from a cell. Cu^+-ATPases are involved in the active pumping of excess copper atoms through the membrane and out of the cell. Mutations in these regulator proteins in humans can lead to disorders such as Menke’s and Wilson’s disease, and imbalance in their regulation is linked to Alzheimer’s disease and resistance to cancer chemotherapy.

Continued on next page…

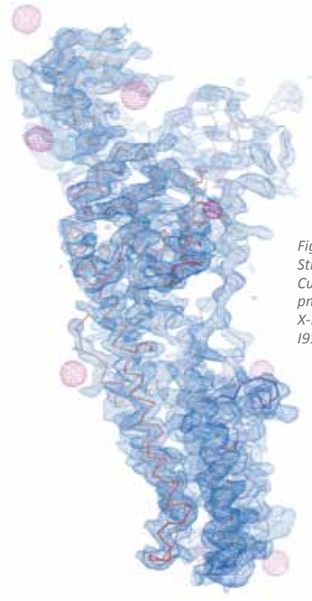

Figure 1.
Structure of the PIB type Cu^+-ATPase from Legionella pneumophila revealed by X-ray crystallography at the I911-3 beamline at MAX-lab.

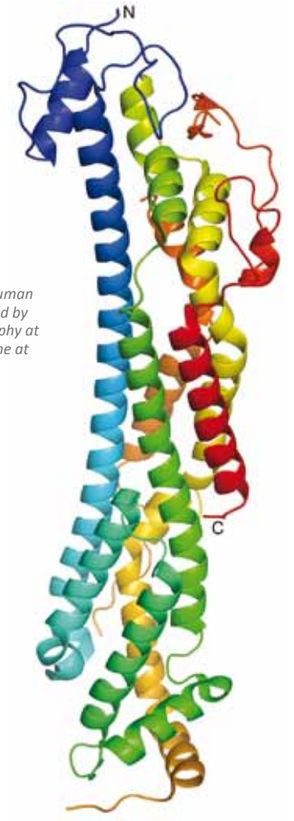

Figure 2.
Structure of the human glypican-1 revealed by X-ray crystallography at the I911-3 beamline at MAX-lab.

A second example is a human protein, glypican-1, that is involved in a variety of cellular signaling processes. In contrast to the Cu^{+}-ATPases, glypicans are not deeply embedded in cellular membranes but are anchored to them through a long flexible tail that has a fatty part at its extremity, which inserts into the membrane. Glypicans constitute a family of similar proteins with six members. By binding to a variety of proteins outside the cell, they are responsible, directly or indirectly, for the transmission of important information into the cell. Several glypicans are responsible for correct morphological development in vertebrates, i.e. the proper formation of different parts of the body. Mutations in glypicans are associated with disease, for example Simpson-Golabi-Behmel syndrome, characterised by prenatal and postnatal overgrowth, and omodysplasia-1, a congenital disease affecting the skeletal system.

Until last year no structural information was available for any member of the glypican family. In particular it was a mystery why every glypican across all species where they are found had 14 conserved cysteine residues. The structure of human glypican-1 was determined completely using data from station I911-3 [2], which together with a structure of a glypican from fruit flies published a few months earlier confirmed that all glypicans will have the same elongated, rod-like structure held together partly by seven disulphide bonds involving the 14 conserved cysteines. A structure which gives great stability to the molecule. By mapping known disease-causing mutations onto the conserved structure it is now possible to understand how these mutations affect the structure and function of the glypicans.

Glypicans belong to the family of molecules known as proteoglycans, which are characterised by consisting of a large proportion of carbohydrate. This was removed in the present study to make crystallisation easier. The carbohydrates are attached in large flexible chains to residues on the surface of the protein, in the flexible tail that is not seen in the crystal structure. Carbohydrate attachment, removal and recycling are important for the function of glypicans. The exact type of carbohydrate that is attached affects the function greatly. The structure of a loop on the surface of glypican-1 offered clues as to why one particular kind of carbohydrate is exclusively attached to this protein. Future structural studies will focus on the mechanisms by which this happens. ■

Part of the data that made it possible to look at a prototype of this protein from a micro-organism at atomic detail was collected at the I911-3 beamline. Careful inspection of the structure, combined with biochemical knowledge, made it possible to suggest the manner in which the copper atoms are transported across the membrane. In particular a hitherto unknown docking platform could be described which may be important for the binding of soluble Cu carrying proteins. This platform could be the gateway for Cu delivery or auto-regulation. Furthermore, by mapping human mutations linked to disease to the structure, regions that are of physiological importance could be identified. These findings can help to better understand Menke's or Wilson's diseases, and it enables the development of new therapies for these diseases. Furthermore, since this type of regulator is very important for all cells, including pathogenic bacteria, influencing its function could lead to the destruction of cells. By a careful analysis of the structures of specific Cu^{+}-ATPases from pathogenic bacteria, new types of antibiotics could be developed, which would be a new weapon in the fight against rising antibiotic resistance.

References:

1. P. Gourdon, X. Y. Liu, T. Skørringe, J. P. Morth, L. Birk Møller, B. Panyella Pedersen, P. Nissen, Nature 475, 59 (2011).

2. G. Svensson, W. Awad, M. Håkansson, K. Mani, D. T. Logan, J. Biol. Chem. 287, 14040 (2012).

HEDGEHOG SPIN TEXTURE AND BERRY'S PHASE TUNABILITY

The behaviour and texture of magnetic spins on surfaces are at present one of the core interests of condensed matter physicists. A collaboration led by the Princeton Hasan team has for the first time, aided by measurements at the I3 beamline at MAX-lab and other facilities, observed a unique hedgehog-like spin texture on the surfaces of manganese-doped Bi_2Se_3 thin films.

Continued on next page...

S.-Y. Xu[a], M. Neupane[a], C. Liu[a], D. Zhang[b], A. Richardella[b], L. A. Wray[a,c], N. Alidoust[a], M. Leandersson[d], T. Balasubramanian[d], J. Sánchez-Barriga[e], Oliver Rader[e], G. Landolt[f,g], B. Slomskif,[g], J. H. Dilf,[g], J. Osterwalder[g], T.-R. Chang[h], H.-T. Jeng[h,i], H. Lin[i], A. Bansil[j], N. Samarth[b] and M. Z. Hasan[a,k]

a. Joseph Henry Laboratory, Department of Physics, Princeton University, New Jersey, USA
b. Department of Physics, The Pennsylvania State University, Pennsylvania, USA
c. Advanced Light Source, Lawrence Berkeley National Laboratory, California, USA
d. MAX IV Laboratory, Lund University, Sweden
e. Helmholtz-Zentrum Berlin für Materialien und Energie, Elektronenspeicherring BESSY II, Berlin, Germany
f. Swiss Light Source, Paul Scherrer Institute, Switzerland
g. Physik-Institute, Universitat Zurich-Irchel, Switzerland
h. Department of Physics, National Tsing Hua University, Hsinchu, Taiwan
i. Institute of Physics, Academia Sinica, Taipei, Taiwan
j. Department of Physics, Northeastern University, Boston, Massachusetts, USA
k. Princeton Center for Complex Materials, Princeton Institute for Science and Technology of Materials, Princeton University, New Jersey, USA

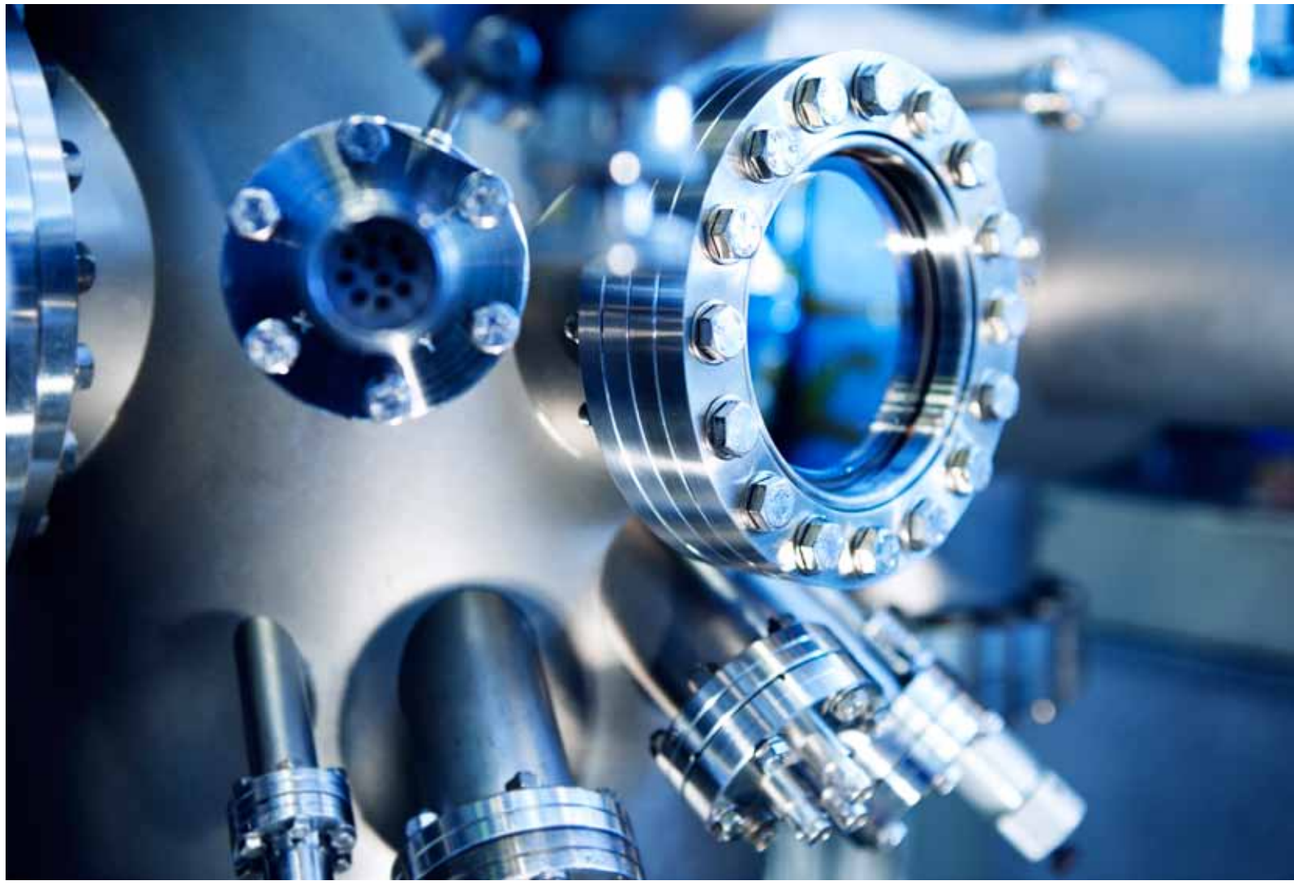

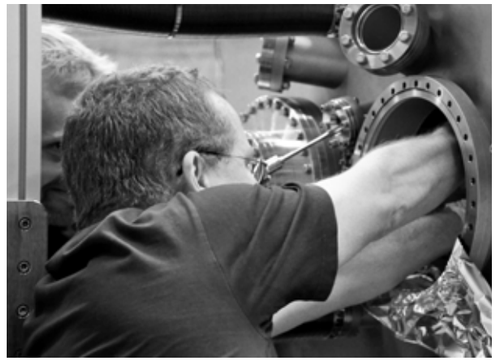

Three-dimensional topological insulators, first experimentally observed and reported in 2007 by the Princeton Hasan team, have attracted huge interests from researchers all over the world. Understanding and controlling spin degrees of freedom on the surfaces of topological insulators are key to future applications as well as for realising novel physics such as the axion electrodynamics associated with time-reversal (TR) symmetry breaking on the surface.

The most recent spin-resolved studies performed at the I3 beamline at MAX-lab (and several other laboratories around the world) led by the Hasan team have, for the first time, experimentally demonstrated magnetically induced spin reorientation phenomena simultaneous with a Dirac-metal to gapped-insulator transition on the surfaces of manganese-doped Bi_2Se_3 thin films. The resulting electronic groundstate exhibits unique hedgehog-like spin textures at low energies, which directly demonstrate the mechanics of TR symmetry breaking on the surface. These spin phenomena and the control of their Fermi surface geometrical phase (the Berry's phase) first demonstrated in these experiments pave the way for the realisation of many predicted exotic magnetic phenomena of topological origin.

Since the discovery of three-dimensional topological insulators, topological order proximity to ferromagnetism has been considered as one of the core interests of the field. Such interest is strongly motivated by the proposed TR breaking topological physics such as quantized anomalous chiral Hall current, spin current, axion electrodynamics, and inverse spin-galvanic effect, all of which critically rely on finding a way to break TR symmetry on the surface and utilise the unique TR broken spin texture for applications. The experimental spin behavior of surface states under the doped magnetic groundstate is thus of central importance to the entire field.

In order to understand the nature of electronic and spin structure in the magnetic topological groundstate vital for magnetic topological devices, an international team lead by the Princeton group, in collaboration with the MAX IV Laboratory in Lund, Sweden and several other laboratories around the world, have utilized spin resolved angle-resolved photoemission spectroscopy at the I3 beamline at the MAX III ring (as well as beamlines in other laboratories) and systematically mapped the momentum-space spin configurations in magnetically doped, non-magnetically doped, and ultra-thin quantum coherent topological insulator films. The evolution of topological surface states with magnetic (Mn) and nonmagnetic (Zn) doping is reported in this research (Figure 1a and b).

More importantly, the spin configuration of the magnetic topological insulator (Mn2.5%-Bi_2Se_3) is revealed by the critical spin-resolved measurements at I3 beamline (see Figure 1c-e for a set of representative spin-resolved measurements). An exotic hedgehog-like spin configuration for each upper (or lower) Dirac band separated by the magnetic gap, which is dramatically reoriented with respect to the helical spin texture on the surface of a TR-invariant topological insulator, has been observed in the measurement. These spin measurements serve as the most direct and concrete evidence of TR symmetry breaking on the surface of a topological insulator, which has been critically lacking in topological insulator research to this date.

The geometrical phase (also known as Berry's phase) bears a direct correspondence to the bulk topological invariant realized in the bulk electronic band structure via electronic band inversion. On the surface of a normal TR-invariant topological insulator (in absence of magnetic doping or impurities) its robust π Berry's phase is the key signature of quantum entanglement of the electronic wavefunction over the macroscopic crystal. Now in the case of TR-broken topological insulator (Mn-Bi_2Se_3 films), as shown by the Princeton-MAX IV Laboratory collaboration in the current research, the Berry's phase behavior is found to be even more exotic: a continuously tunable (π to 0) Berry's phase is realized by the observed hedgehog-like spin texture. Chemical or electrical gating on the surface (e.g. demonstrated by surface NO_2 adsorption in Figure 1a and b) of Mn-Bi_2Se_3 leads to such Berry's phase tunability.

Relevant research funding: (Princeton Univ.) U.S. Department of Energy (DOE), Office of Basic Energy Sciences (BES); (The MAX IV Laboratory) The Swedish Research Council, The Knut and Alice Wallenberg Foundation, the Swiss Light Source, the Swiss National Science Foundation. Funding source of other laboratories can be found in the publication.

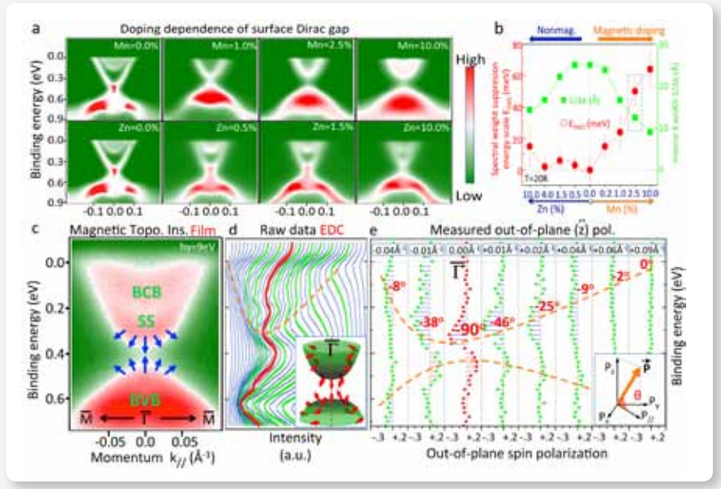

Figure 1.
Hedgehog spin texture on the surface of magnetic doped topological insulator.
(a) Electronic band dispersion of Mn(Zn)-doped Bi_2Se_3 MBE thin films along the – – momentum space cut.
(b) The Dirac point spectral weight suppression (SWS) energy scale E_{SWS} and inverse momentum width 1/Δk of the surface states are shown as a function of Mn and Zn concentration measured at T=20 K.
(c-e) Spin Measurements on Mn (2.5%) film at the I3 beamline.

References:
S. - Y. Xu, M. Neupane, C. Liu, D. Zhang, A. Richardella, L. A. Wray, N. Alidoust, M. Leandersson, T. Balasubramanian, J. Sánchez-Barriga, O. Rader, G. Landolt, B. Slomski, J. Hugo Dil, J. Osterwalder, T. - R. Chang, H. -T. Jeng, H. Lin, A. Bansil, N. Samarth, M. Z. Hasan, Nat. Phys. 8 616 (2012).

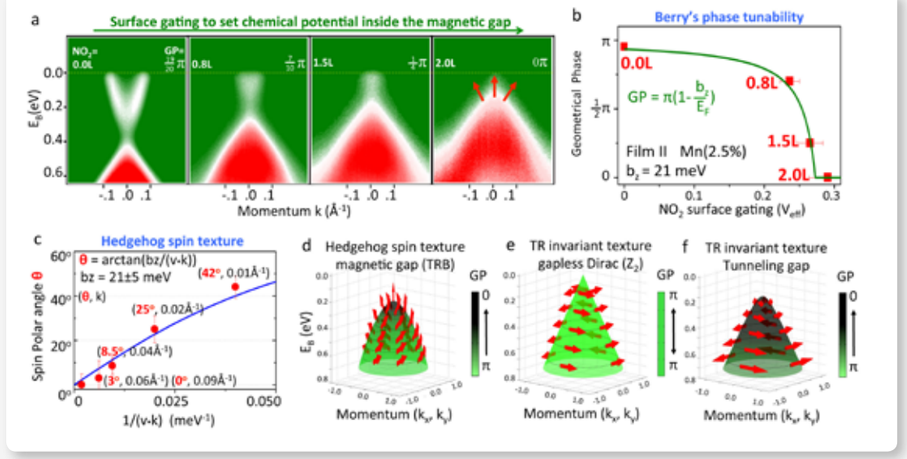

Figure 2.
Berry's phase tunability on a magnetic topological insulator surface.

(a) Surface state dispersion measured on in-situ NO_2 surface adsorption on the Mn-Bi_2Se_3 surface. The NO_2 dosage in Langmuir units ($1L=1\times10^{-6}$ torrs) and the tunable geometrical phase (GP) (or the Berry's phase) associated with the topological surface state are noted on the top-left and top-right corners of the panels, respectively.

(b) GP associated with the spin texture on the iso-energetic contours on the Mn-Bi_2Se_3 surface as a function of effective gating voltage induced by NO_2 surface adsorption. Red squares represent the GP experimentally realized by NO_2 surface adsorption, as shown in a. GP=0 (NO_2=2.0 L) is the condition for axion dynamics.

(c) The magnetic interaction strength bz, which corresponds to half of the magnetic gap magnitude, is obtained on the basis of spin-resolved data sets (polar angle ϑ, momentum k) for Mn(2.5%)–Bi_2Se_3 film II (see Figure 1).

(d) The TR breaking spin texture features a singular hedgehog-like configuration when the chemical potential is tuned to lie within the magnetic gap, corresponding to the experimental condition presented in the last panel in a.

(e, f) Spin texture schematic based on measurements of Zn-doped Bi_2Se_3 film (60 QL), and 3 QL undoped ultra-thin film with the chemical potential tuned to the Dirac point energy or within the tunneling gap.

AMBIPOLAR DOPING IN GRAPHENE CONTROLLED BY GE INTERCALATION

K. V. Emtsev[a], S. Forti[a], A. A. Zakharov[b], C. Coletti[a,c] and U. Starke[a]

a. Max-Planck-Institut für Festkörperforschung, Stuttgart, Germany
b. MAX IV Laboratory, Lund University, Sweden
c. Center for Nanotechnology Innovation @ NEST, Istituto Italiano di Tecnologia, Pisa, Italy

Graphene – carbon atoms in one single layer – is an exciting material that can be thoroughly examined in synchrotron light facilities. One challenge is to get a large, homogeneous graphene layer and dope it both with electrons and holes. Here experiments with germanium to meet that challenge are presented.

Epitaxial graphene layers on SiC (0001) are coupled to the substrate by an interface layer that induces a strong n-doping in the graphene. An elegant way to circumvent this influence of the interface is to break the covalent bonds via atomic intercalation [1]. As a result, large scale, homogeneous, quasi-free standing graphene layers can be achieved [2]. Here we report on the intercalation of germanium, by which the electronic structure of the decoupled graphene can be tailored. Two symmetrically doped, namely n- and p-type phases are stabilized, depending on the amount of intercalated Ge. By preparing the two phases in coexistence, lateral p-n junctions can be formed on a mesoscopic scale [3]. For this project, low energy electron and photoemission microscopy (LEEM/PEEM) investigations were carried out at the ELMITEC III instrument at beamline I311 of the MAX II ring at MAX-lab.

Ge is deposited in ultra-high vacuum (UHV) on to a zero layer graphene (ZLG) sample on SiC(0001), i.e., on the initial carbon layer that serves as interface and itself does not possess a delocalized π-band [4]. Subsequent annealing leads to the intercalation of an atomically thin Ge film underneath the ZLG (see inset sketches in Figure 1). The covalent bonds between the carbon atoms in the ZLG and the topmost Si atoms of the SiC substrate are broken upon the in-diffusion of Ge atoms, i.e., the interface bonding is lifted and the ZLG layer is structurally decoupled from the SiC surface as revealed in Figure 1 by X-ray photoemission (μ-XPS). The two components S1 (S2) in the ZLG data representing carbon atoms with (without) covalent bonds to the SiC substrate are converted to a sharp peak (G) corresponding to free-standing graphene.

Angle-resolved photoemission spectroscopy (ARPES) reveals that after the Ge intercalation, the former ZLG layer exhibits the Dirac-like band structure of graphene, as demonstrated in Figure 2. As shown in panels (a) and (c), a distinct p- or n-doping can be achieved by using different annealing temperatures. After an initial deposition of approx. 5 monolayers (ML) of Ge, the p-phase arises from annealing at 720°C, while the n-phase develops after further heating to 920°C. Structurally, the two phases of different doping are characterized by a different amount of intercalated Ge, as deduced from Ge 3d core level emission intensities in XPS (not shown). Consistently, the n-phase can also be prepared directly by depositing a smaller Ge amount and annealing to 720°C. Notably, during the transition between the two phases, a coexistence of the p- and n-doped graphene regions is observed, as displayed in Figure 2b. However, the doping level for the two phases is fixed as can be seen by the persistent sharpness and energy position of the two π-band branches observed in several experiments. This necessarily means that, at this stage, the surface splits into coexisting p- and n-patches which suggests the presence of lateral graphene p-n junctions (see below).

Insight into the mechanism of the germanium penetration can be obtained by LEEM measurements carried out *in-situ* during the annealing process (30 sec. time steps). As shown in Figure 3a-c the intercalation process proceeds fast over a complete terrace, while at the terrace edges it is kinetically limited. Figure 3d shows microscopic details of the transformation after quenching the surface during the intercalation process. Contrast differences reveal three characteristic areas that can be identified by μ-LEED snapshots. The dark area with the (6√3 x 6√3)R30° pattern (panel e) corresponds to an unconverted ZLG (covered with Ge). The bright area (panel f) is fully converted and shows the graphene (1×1) diffraction pattern. Panel (g) – obtained from the greyish area – displays a superposition of the (1×1) and ZLG patterns. This transition region consists of densely packed grains (≈ 50 nm) where, presumably, the germanium is already intercalated and covered with graphene islands, and which gradually coalesce into a continuous graphene layer.

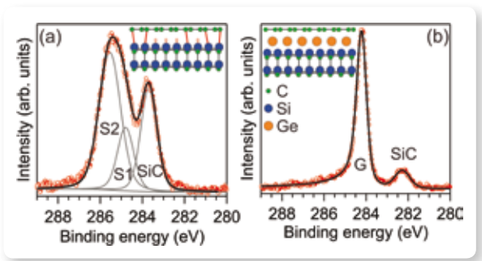

Figure 1.
C1s core level spectra (a) from the initial ZLG on SiC(0001) and (b) after deposition of 5 ML of Ge followed by vacuum annealing at T=720°C (Photon energy: 380 eV, structural models sketched in the insets). Experimental data are shown as open (red) dots, fitted by the solid (black) lines. In panel (a) the fitted components are also shown (grey lines).

The transition from p- to n-phase graphene proceeds in a different manner. The spatial distribution of the differently doped patches is investigated by LEEM and PEEM in this transition stage. Figure 4a shows a LEEM micrograph of the p-phase Ge-decoupled graphene, obtained after annealing at 720°C, cf. Figure 2a. The graphene layer is quite homogeneous and covers the entire surface. Graphene domains are determined by the size of the SiC substrate terraces, i.e., they are of the order of 3-5 μm in width. Successive stages (shorter and longer annealing) of the emergence of the n-doped graphene phase are displayed in Figures 4b and c, respectively. The corresponding PEEM image in panel (d) reveals a significant contrast in intensity of the Ge 3d core level signal for the two graphene phases. Contrast in PEEM is determined by the concentration of Ge atoms located beneath the epitaxial graphene layer and the spatial distribution coincides with the contrast obtained in LEEM. This corroborates the fact that the n-phase is induced upon a partial desorption of germanium from under the surface, i.e., partial de-intercalation. Surprisingly, the process is not initiated at the step edges but rather on the terraces (see Figure 4b), suggesting a local reaction through the graphene layer, a mechanism that is very different from the common intercalation processes known for graphite. This local process leads to the formation of n-doped graphene islands as small as 100 nm, embedded into the p-doped graphene sheet, so that lateral p-n junctions develop. With further annealing the islands grow in size and coalesce forming extended n-doped graphene areas. ■

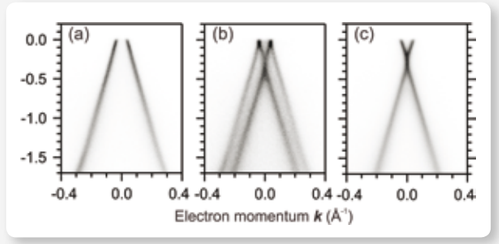

Figure 2.
Photoemission valence band maps vs energy and electron momentum in the vicinity of the $\bar{K}$-point (k=0) of the graphene Brillouin zone (taken parallel to the $\bar{T}\bar{K}$-direction) after deposition of 5 ML of Ge followed by annealing in UHV at (a) T=720°C, (b) 820°C, and (c) 920°C (Photon energy: 90 eV), measured at the Swiss light source (SLS) of the Paul-Scherrer-Institute (PSI) in Villigen, Switzerland.

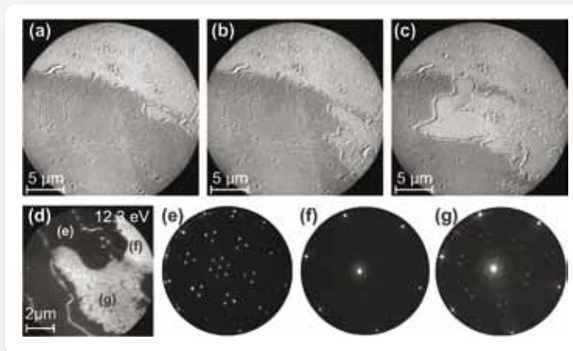

Figure 3.
(a-c) LEEM micrographs obtained during the intercalation of Ge (30 sec. steps). (d) LEEM micrograph after incomplete intercalation (smaller field of view). (e-g) μ-LEED snapshots (43 eV) of the dark, bright and grainy areas of panel (d), as indicated, corresponding to an unconverted Ge covered surface, a fully converted graphene phase and a partially converted area quenched in the transformation process, respectively.

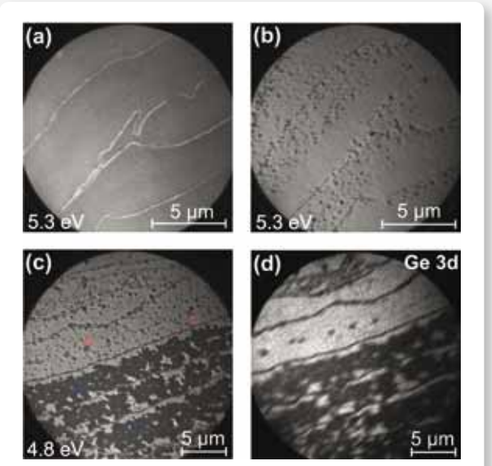

Figure 4.
LEEM micrographs of the decoupled graphene layer obtained by intercalation of Ge atoms at the interface with SiC(0001) surface: (a) homogeneous p-doped graphene phase, and (b) initial stage of the graphene p-n junction formation. Dark inclusions in (b) correspond to the n-doped graphene islands embedded into the p-doped graphene. (c) LEEM micrograph and (d) PEEM Ge 3d intensity map of the graphene p-n coexistence stage. Bright (dark) regions correspond to p-doped (n-doped) quasi-free standing graphene regions.

References:
1 C. Riedl, C. Coletti, T. Iwasaki, A. A. Zakharov, U. Starke, Phys. Rev. Lett. 103, 246804 (2009).
2 S. Forti, K.V. Emtsev, C. Coletti, A.A. Zakharov, C. Riedl, U. Starke, Phys. Rev. B 84, 125449 (2011).
3 K.V. Emtsev, A.A. Zakharov, C. Coletti, S. Forti, U. Starke, Phys. Rev. B 84, 125423 (2011).
4 K.V. Emtsev, F. Speck, Th. Seyller, L. Ley, J.D. Riley, Phys. Rev. B 77, 155303 (2008).

THE NEW MULTIPURPOSE SAXS BEAMLINE AT I911-SAXS

A. Labrador[a], Y. Cerenius[a], K. Theodor[a, b], C. Svensson[a], T. Plivelic[a]

a. MAX IV Laboratory, Lund University, Sweden
b. Niels Bohr Institutet, University of Copenhagen, Denmark

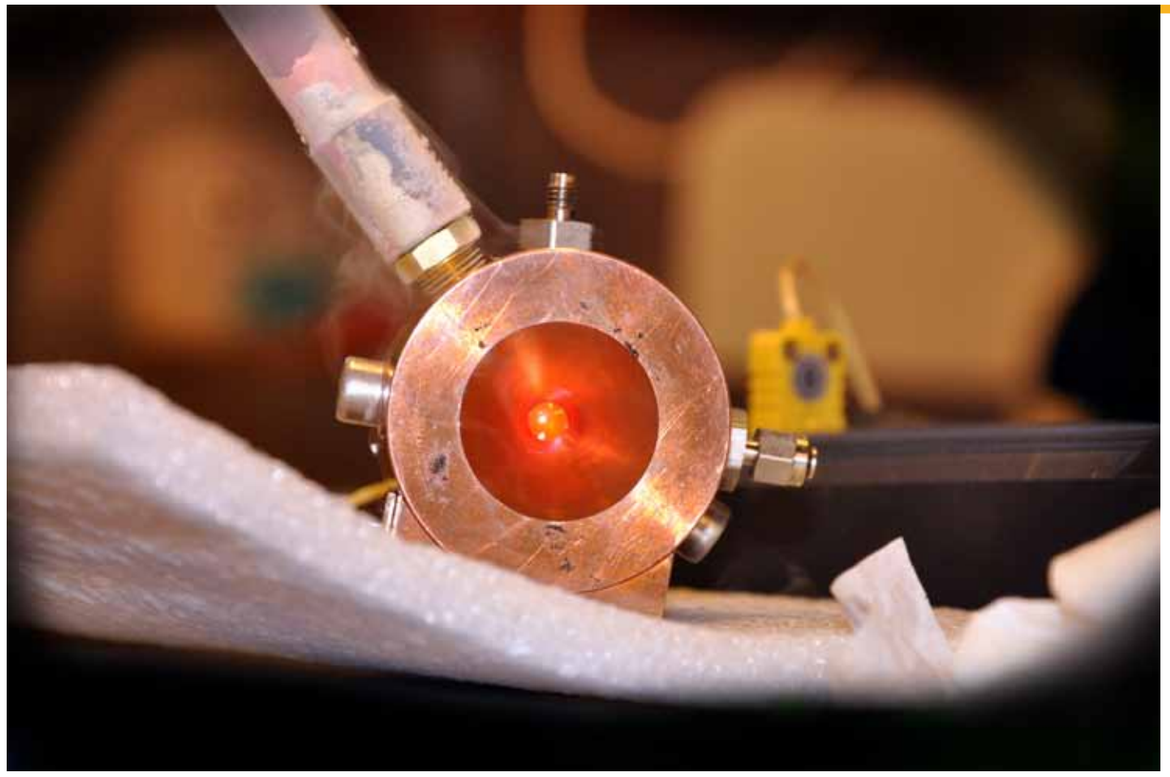

SAXS (Small-Angle X-ray Scattering) has become a key technique to analyse materials at a molecular level. It offers the possibility of studying samples in their own natural environment or under well controlled conditions. Its multidisciplinary applications range from industrial (alloys, ceramics or polymers) to biological systems and cover a wide range of material morphologies and structures.

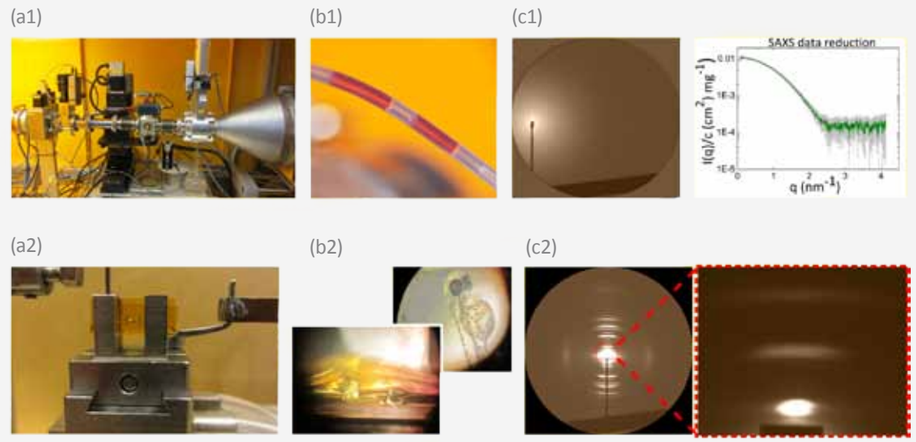

Figure 2.
Illustration of the diversity of setups (a1, a2), samples (b1, b2) and scattering images (c1, c2) at I911-SAXS.
Top: Setup being developed for high-throughput solution scattering using an in-vacuum flow-through capillary (a1) where the protein in solution (b1) is exposed to the X-rays. Image (c1) shows a diffracted image and the corresponding 1D radial integration.
Bottom: A user setup. The cuvette and stretching mechanism (a2) allows muscle contraction studies of zebra fish larvae (b2). The scattered image of collagen from rat tail tendon used as a calibrant is shown in (c2).

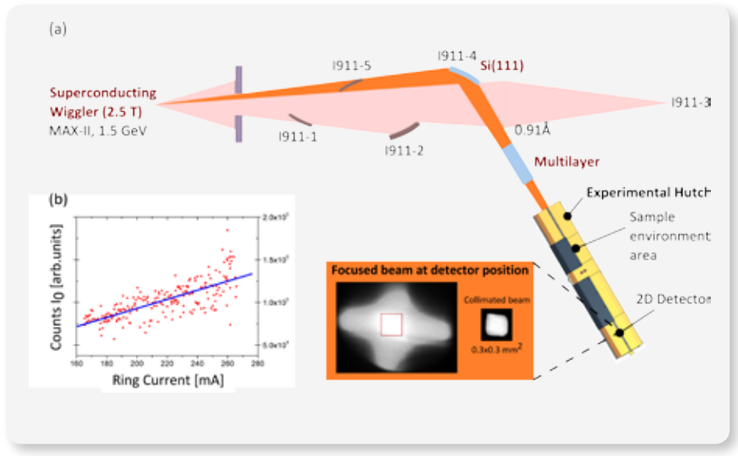

Figure 1.
(a) Schematics of the fan from the I911 wiggler, indicating the part of the beam used at the SAXS station I911-4. The X-rays diffracted by the Si(111) crystal are focused at the position of the 2D detector collecting the scattered X-rays. (b) I_0 value (red dots) after each alignment performed over a 60 hours long, experimental run. The linear fit of I_0 with respect to the ring current (blue line) shows that the intensity decay of the collimated beam is proportional to the ring current.

In 2008 a Swedish-Danish collaborative group took the initiative of converting one of the five Cassiopeia [1] side stations (I911-4) to a dedicated SAXS beamline (I911-SAXS) in view of the increasing demand on beamtime from the SAXS user community at I711. After some preliminary conceptual feasibility tests, a new experimental hutch was constructed to satisfy the experimental requirements of the technique. The final commissioning of the new I911-SAXS station started in autumn 2010 and the station was opened to the user community in May 2011. The shifts for peer-reviewed projects, which correspond to 75% of the total beam delivery time, are currently fully exploited.

Continued on next page...

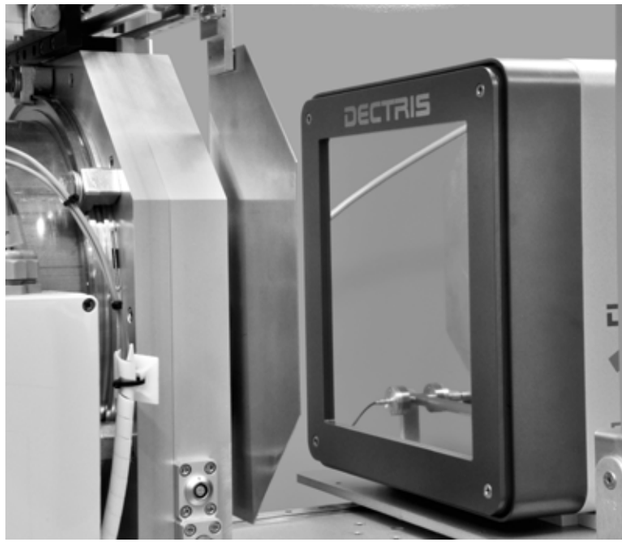

The new SAXS station, uses one side of the central fan of the I911 superconducting multiple wiggler, from 0.5 to 1 mrad (Figure 1a). The fixed wavelength selected by the I911-4 Si(111) monochromator is 0.91 Å. The horizontal and vertical focusing is provided by the meridional bending of the monochromator and by a curved Mo-Si multilayer mirror respectively. The size of the focal spot is about 0.3 x 0.2 mm^2 FWHM (HxV) at the sample position and the flux is estimated to be 5 x 10^{10} photons/s. Measurements with a beam collimated down to 0.1 x 0.1 mm^2 can be performed with good scattering samples. The easy accessible experimental "mini-hutch" [2], which resembles a conventional home-lab SAXS system, is a stainless steel cabinet which encloses the downstream parts of the beamline: the sample experimental area, the evacuated and modular SAXS chamber, the I_0 and I_t counters and the 2D detector to acquire the X-rays scattered by the sample. The whole set-up was conceived to work under pressure up to 10^{-2} mbar. Two sliding doors permit routine access to the sample environment area and for modifications of the SAXS chamber lengths. The sample to detector distance can be changed from a few hundred millimeters to more than 2 meters. A very useful and practical feature of this set-up is the design of the SAXS chamber which allows offsetting the exit window without changing the beamstop position. In this way the q-range (where $q = (4\pi/\lambda)\sin\theta$) can be easily changed without modifying the chamber length. The accessible q-range of a typical I911-SAXS setup is 0.01 $Å^{-1}$ - 0.3 $Å^{-1}$ but lower values (0.006 $Å^{-1}$) or higher (2 $Å^{-1}$) can also be reached.

The optical design of the I911 side stations makes them vulnerable to any change in the monochromator heat load. This induces changes in the intensity I_0, and position of the focused beam which is critical in a collimated beam. A beam alignment procedure has been developed and has extensively proved its reliability. Figure 1b shows the I_0 values after alignments performed over 60 hours during a real experimental run. The users can choose to optimize the beam at any time or schedule it to be automatic before collecting each image or when the intensity has dropped a given percentage.

The low level beamline control system is implemented using Tango middleware (device servers). The experimental logic is coded with SPEC macros and most of the functionality needed for the user to run the experiment, including the beam intensity optimisation routines, is driven with an in-house developed Graphical User Interface. This interface also provides SAXS data reduction and multiple frame processing. On-line data reduction of isotropic and anisotropic SAXS data is under development.

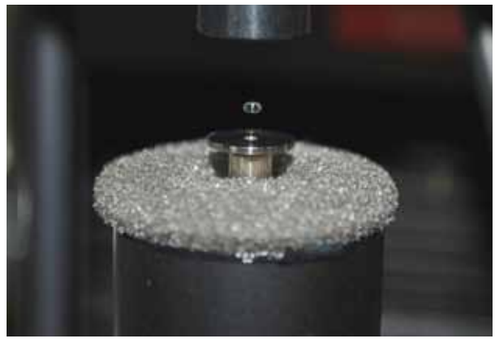

A selection of fundamental SAXS sample environments has been available from day one: an in-vacuum flow-through capillary for solution scattering and several multiple positions sample-holders for solids (films and powders), gels or liquid samples in air. Both systems can be used with a water-bath temperature control. Other setups, brought by the users, are often installed and integrated into the beamline such as ultrasonic levitators, electrochemical cells or a tensile test machine. Currently, the continuous requests and feedback from the user community is contributing to further development of *in-situ* and time resolved I911-SAXS experiments (Figure 2).

In conclusion, the new SAXS beamline at the MAX IV Laboratory has fully replaced, improved and expanded the SAXS activities at I711. The optimized experimental conditions at I911-4 result in more than 10 times higher photon flux on the sample when measured under similar conditions. An important feature for the beamline performance is the beam alignment automation routine, which easily maximizes the beam intensity during data collection. So far, there have been successful measurements, in a resolution range from few to hundred nanometers, on a diversity of samples and setups mostly oriented to soft matter and protein in solution experiments. Recently a low noise, fast read-out pixel detector (PILATUS 1M) has been acquired and commissioned and is already available for the user community. ■

References:

1. C. B. Mammen, Design and construction of the Cassiopeia beamline for protein crystallography at MAX- lab, Lund. Ph.D. thesis 2005. M. Thunnissen, J. Als-Nielsen, AIP Conf. Proc. 705, 808 (2004).

2. A. Labrador, Y. Cerenius, C. Svensson, K. Theodor, C. Svensson, J Nygaard, T. Plivelic, J. Phys.: Conf. Ser., under review.

FEL – TESTS TODAY AND OUTLOOK FOR TOMORROW

The scientists of the MAX IV Laboratory and their collaborators are already looking into the future, beyond MAX IV. The next generation of light sources is Free Electron Lasers (FEL) and MAX IV is being prepared for that development through the construction of a test free electron laser at MAX-lab.

The MAX IV facility is in the construction phase, but already ideas are taking form of how it can be developed in the future with an X-ray FEL. Tests and development of FEL techniques have been on-going for several years in a test FEL facility at MAX-lab. Collaborations with other laboratories have been built and recently a joint map for the scientific case and development of FELs in Sweden has been drawn together with the FEL center Stockholm-Uppsala and the major universities in Sweden.

The FEL is the main technique to create coherent, extremely intense and very short light pulses in the X-ray range. Recently the LCLS at Stanford and the SACLA in Japan have been put into operation generating radiation down to 1 Å at GW power levels in sub 100 fs pulses. The idea of incorporating a FEL at the MAX IV facility was present already in the early designs and the linac injector is now prepared to be able to drive a FEL in the future.

The FEL poses new questions that demand the development of novel experiences. One major step has been the decision to build the test FEL at MAX-lab. The aim is to investigate different FEL techniques with a focus on seeding, gain experience and use it as a platform for collaboration, development and education. The activities have been performed in collaboration with the Lund Laser Center (LLC) and Helmholtz Zentrum Berlin (HZB).

The test FEL facility

The test FEL facility at MAX-lab was built during the first Eurofel collaboration (financed by EU under FP6) in collaboration with HZB in Berlin. Laser expertise was provided by the LLC from the early stages of development. The facility is based on the current MAX-lab injector which was complemented with a double laser system (gun and seed), two undulators, chicanes for laser injection and pulse compression, and an optical diagnostics beamline. It is a seeded FEL working in Coherent Harmonic Generation (CHG) mode, and coherent radiation from the fundamental (1st harmonic at 263 nm) to the 6th harmonic (45 nm) in linear mode (see

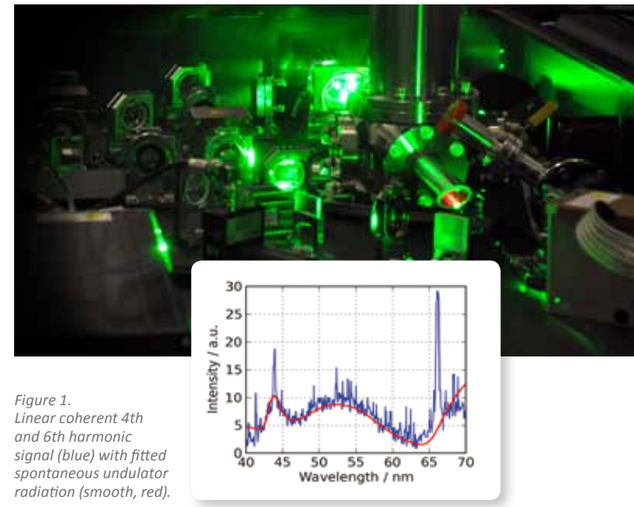

Figure 1. Linear coherent 4th and 6th harmonic signal (blue) with fitted spontaneous undulator radiation (smooth, red).

Figure 1) was produced already in 2010 [1]. The second and fourth harmonics have also been recorded in helical mode.

Coherence and polarization measurements

The test FEL at MAX-lab is capable of generating light with high coherence, both longitudinally and transversely, and tunable helicity. The longitudinal coherence is manifested by the existence of a coherent enhancement in the signal (Figure 1). The transverse coherence has been investigated in 2011 [2] by a series of double slit measurements. Four different double slit apertures were tested, with slit widths of 40 µm and 100 µm and slit separation of 400 µm and 800 µm. The slits were cut by a laser into a thin steel foil.

Figure 2 (top) shows the CCD image recorded at the spectrometer for the smallest double slit sample (40 µm slit width and 400 µm slit separation) and Figure 2 (bottom) shows the intensity in the vertical direction of the beam together with a theoretical fit. From the theoretical fitting, the fringe visibility is found to be v = 0.67. However, the beam is expected to have a much higher degree of coherence as the shot-to-shot instabilities deteriorate the signals.

The polarization state of the coherent signal has been measured [2] using a Rochon prism polarizer made of magnesium fluoride (MgF_2), which has a transmission of about 30% at 131 nm. The CHG radiation in the second harmonic was found to be significantly elliptical with an ellipticity of 0.38 and ellipse rotation of 41 degrees. The ellipticity can be explained by the electron beam not following the axis of the APPLE-II undulator. The rotation suggests a phase retardation of the vertical or horizontal polarization components in the beamline.

Continued on next page...

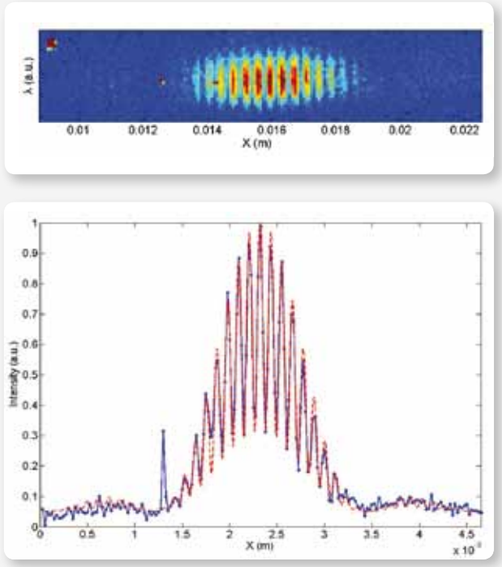

Figure 2.
Double slit diffraction. Top: CCD image of the diffraction pattern. Bottom: Line out of the pattern.

Figure 3.
The HHG gas jet chamber.

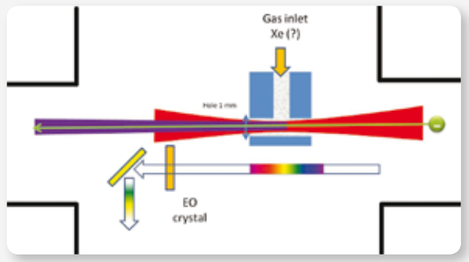

Figure 4.
Schematics of the gas jet chamber with drive laser and electrons entering from the right. A co-propagating laser beam for timing diagnostics using an EO crystal at the bottom.

References:
1. N. Cutic, F. Lindau, S. Thorin, S. Werin, J. Bahrdt, W. Eberhardt, K. Holldack, C. Erny, A. L'Huillier, E. Mansten, PRSTAB 14, 030706 (2011).

2. J. Schwenke, E. Mansten, F. Lindau, N. Cutic, S. Werin, , Proceedings of the International Free Electron Laser conference, Shanghai (2011).

CURRENT STATUS OF THE MAX IV LABORATORY

Francesca Curbis[a], Nino Cutic[a], Filip Lindau[a], Erik Mansten[a], Olivia Karlberg[a], Sverker Werin[a], Fernando Brizuela[b], Christoph Heyl[b], Anne L'Huillier[b], Byunghoon Kim[b], David Kroon[b], Jörg Schwenke[c], Johannes Bahrdt[d], Karsten Holldack[d]

a. MAX IV Laboratory, Lund University, Sweden
b. LLC/Division of Atomic physics, Lund University, Sweden
c. University College London, UK
d. Helmholtz Zentrum Berlin, Berlin, Germany

HHG seeding

It is of great interest to extend the seeding technology to shorter wavelengths. The two main techniques explored are laser seeding with an external laser and self-seeding, where the radiation is filtered in a monochromator before further amplification. In the range 40-200 nm the most promising laser source available for seeding is High Harmonic Generation (HHG) in gas.

The test FEL facility is now being rebuilt to explore a HHG source at 100 nm, its influence on accelerator operation and seeding capabilities. A major concern is to transport the high harmonic generated in the gas to the electron beam in the first undulator. The test FEL will utilize an extremely compact design where the gas jet chamber (Figure 3) is placed inside (Figure 4) the accelerator system and both the drive laser and the electrons pass the gas. Despite the basic simplicity it poses new issues. Among them are:

- The electron beam, the seed laser and the pump laser need to co-propagate.
- The electron beam may disturb the HHG process in the gas.
- The electron beam emittance may be deteriorated by the gas.
- The HHG seed consists of an attosecond pulse train, not a full wave.

Collaborations and outlook to the future

To run the FEL technology development, in both a MAX IV perspective and a broader scope, close collaborations have been built especially with the LLC, but also with the HZB, Berlin. The test FEL was built under the European collaboration Eurofel (FP6) which is now entering a new phase; "EuroFEL". A MoU was recently signed between the major FEL laboratories in Europe for continued joint development.

A road-map for the development of FELs in Sweden has been developed in collaboration with the FEL centre Stockholm-Uppsala and the major universities in Sweden. A scientific case will be elaborated jointly and design studies will be performed for an FEL on MAX IV, in a time perspective within 10 years, and an FEL in Stockholm-Uppsala in a longer perspective.

An FEL requires an electron beam with higher quality (emittance, peak current and energy spread) than the injection to the storage rings of MAX IV. The linear accelerator on MAX IV will soon be commissioned and following that a project has started in which the system will be studied and tuned to adapt for future FEL operation. ■

MAX-lab RINGS AND ACCELERATORS

The MAX IV Laboratory has more than 25 years of experience of developing accelerators and storage rings for synchrotron radiation and nuclear physics experiments. The first ring MAX I was built on location at MAX-lab in the early 1980's and started operating in 1986. With the additions of MAX II in 1996 and MAX III in 2007 the laboratory has grown into a world renowned facility for internationally competitive nuclear and synchrotron research.

All three rings at MAX-lab are used for synchrotron radiation production and the MAX I ring is also used as a pulse-stretcher for experiments in nuclear physics. The three rings are fed by the 400 MeV MAX injector installed in 2002. The table on page 47 gives an overview of the machine parameters of the accelerators and rings at MAX-lab.

MAX I

MAX I was initially intended for nuclear research only, but was eventually designed also for synchrotron light experiments and has played a prominent role in stimulating and developing Swedish synchrotron light research. With a circumference of 32.4 meters it is the smallest storage ring at MAX-lab and as it is equipped with only one insertion device, synchrotron light is mostly produced by the dipole magnets.

The MAX I ring is aging and suffers from reduced beam life-time in the storage mode due to vacuum problems. Today most synchrotron light research has moved over to the newer and more advanced MAX II and MAX III which have better performance and since only two synchrotron light experiments remain on the ring a vacuum upgrade is of lower priority.

When MAX I is used as a synchrotron light source it is filled up with electrons with an energy of 200 MeV after which they are accelerated up to 550 MeV. The emittance for MAX I is 40 nmrad.

In the pulse-stretching mode for nuclear physics, the deterioration of the vacuum system is of no importance. The properties of the electron beam are for this application now rather close to the design values and both the ring and injector are working under stable conditions. Efforts to extend the operational energy range are on-going.

MAX II

MAX II is a third generation synchrotron source and with a circumference of 90 meters it is the largest ring at MAX-lab. It started operation in 1996 and as it has taken over many of the experiments previously offered at MAX I it is the most intensely used storage ring.

The energy of the electrons entering MAX II from the injector is 400 MeV. The electrons are then accelerated inside the storage ring until they reach 1500 MeV. MAX II has an emittance of 9 nmrad and has seven insertion devices.

The MAX II ring was working very well during the entire 2011, exceeding the mean current and availability figures from 2010. The electron beam stability is in the micrometer range and beam position movements due to the polarization bump excitation are significantly lower than before. 270 to 300 mA are injected twice a day and the beam life-time is 4-6 Ah with some 170 mA remaining at each new injection. The mean current is now typically above 200 mA.

On average, 8% of the total time is spent on injection and ramping of the lattice magnets, undulators and the superconducting wigglers. Significant down-time only occurred during four of the forty user weeks of 2011, see Figure 2 in Facts and Figures. The down-time was mainly due to errors or thunderstorms occurring during weekends, when the "key" person could not always be available.

MAX III

MAX III is MAX-lab's youngest storage ring and was built to both unburden MAX II and replace MAX I for synchrotron light research in the ultraviolet and infrared wavelengths. It has a circumference of 36 meters, two insertion devices and an emittance of 13 nmrad. In MAX III electrons are injected at 400 MeV and are then accelerated up to 700 MeV for production of synchrotron light.

MAX III was also built to test a whole new magnet technology which will be used at MAX IV in the future, see the chapter *The MAX IV Accelerator Project.* The magnets in MAX III are in contrast to the magnets in MAX I and MAX II very compact and are combining several functions in one magnet. Examples include magnets that can be used in both dipole and quadrupole mode.

The MAX III ring is operating with three beamlines. Availability during 2011 was typically around 95 % over the first three quarters of the year, with 3 % of the total time taken away by injections and 2 % by down-time, see Figure 2 in Facts and Figures. Installation of a Landau cavity during week 42 led to some reduction in availability. The remaining weeks of the year an average of 90 % availability was reached. The mean current during this period was quite low partly due to a vacuum leak in the newly installed IR beamline and partly depending on an insufficient vertical beam emittance blow-up.

The MAX Injector

The MAX injector delivers electrons to the three storage rings at MAX-lab and the free electron laser (FEL). Electrons are produced in an electron gun and are then accelerated in the linear accelerator. The injector can send out pulses with electrons up to ten times per second.

The injector is of a recirculated linac type and consists of an RF gun and two S-band linac sections 5.2 meter long equipped with SLED cavities. A recirculation magnet system is used to double the electron energy. The linac sections are now conditioned to a little more than 100 MeV energy gain each and the maximum energy gain for both linacs is 210 MeV. By recirculating the electron beam once through the linacs a maximum electron energy of 420 MeV can be reached.

The RF electron gun used for injection is equipped with a thermal cathode. This gun is quite reliable, but the beam quality is rather poor, due to space-charge effects during the early acceleration in the gun. The performance of this thermionic gun is however quite sufficient for injection into the rings. For the FEL runs, the thermionic BaO cathode is used as a laser-driven photo-cathode.

The MAX injector has been quite reliable during 2011 and negligible time has been lost due to malfunctioning of the accelerator.

The test Free Electron Laser at MAX-lab has produced its first light. The system is built around the MAX injector utilizing two undulators placed inside the MAX II storage ring. The system is seeded by a 263 nm Ti:Sapphire laser and can produce fully coherent radiation in harmonics of the seed. For further information, see the scientific highlight *FEL - Tests today and outlook for tomorrow.* ■

Machine Parameters

MAX INJECTOR LINAC	
Max energy	420 MeV
Pulse current	50 mA
Pulse length	50 ns
Energy spread	Not verified
Emittance	Not verified
MAX I RING	
Storage mode:	
Max energy	550 MeV
Max circ current	300 mA
Hor emittance	40 nm rad
RF	500 Mhz
Bunch length (FWHM)	80 ps
Beam life-time	4 h (Now decreased to some 2 h)
Pulse-stretcher mode:	
Electron energy	144, 188 MeV
Duty factor	75 %
Stretched pulse current	20 nA
MAX II RING	
Max energy	1.5 GeV
Max circ current	290 mA
Hor emittance	8.8 nm rad
RF	100 MHz
Beam life-time	5-6 Ah (25-30 h at 200 mA)
MAX III RING	
Max energy	700 MeV
Max circ current	300 mA
Hor emittance	14 nm rad
RF	100 MHz
Beam life-time	1-1.5 Ah

MAX-lab BEAMLINES

There are currently 20 beamlines in operation at the three MAX-lab rings. The majority of the beamlines (14) are installed at the MAX II ring, while three beamlines for measurements in the ultraviolet and infrared are installed at the newer MAX III. Only two beamlines for synchrotron experiments and one for nuclear physics are still in operation at the aging MAX I. For a detailed description of the beamlines see below and tables 1, 2 and 3.

Main achievements during 2011 include the installation and commissioning of the new end-station on beamline I511-1 for high pressure photoemission measurements, the new SAXS station on I911-4 and the new infrared spectromicroscopy beamline D7 on MAX III. See the scientific highlights in this report for more details.

During 2011 more personnel were hired in both the scientific and technical staff to improve the beamline development and maintenance work as well as the general user support.

MAX I Beamlines

Beamline 41 is used for angle resolved photoelectron spectroscopy on solids in the photon energy range from 15 to 200 eV using a toroidal grating monochromator (TGM). The beamline is suited for measurements of both valence bands and shallow core levels. The experimental station consists of an analyser chamber with a goniometer mounted electron energy analyser (VSW HA50), a sample storage chamber and a sample introduction chamber. The analyser chamber is equipped with LEED, ion sputtering gun, gas-inlet system and a number of optional ports for user owned sample preparation accessories. In addition to this basic set-up a molecular-beam epitaxy (MBE) system with six Knudsen cells and a RHEED optics is available for the growth and *in-situ* studies of III-V compound semiconductors.

Table 1.
MAX I Beamlines

Beam port	Source type	Beamline / Monochromator	Energy or wavelength range	Experimental techniques
41	Bending magnet 18 mrad	4.7m-TGM, 162°.	15 - 200 eV	Angular resolved photoemission. On-line MBE system.
73	Bending magnet 60 x 100 mrad^2	Two ellipsoidal mirrors, 1:1	12000 - 10 cm^{-1}	Infrared microspectroscopy (moved to D7 on MAX III in Sept. 2011). Infrared spectroscopy using a high resolution FTIR spectrometer.
NP	Tagged photon beam	Tagging spectrometer	15 - 185 MeV	Nuclear physics.

Beamline 73 is used for spectroscopy and microscopy in the far, mid and near infrared region (10-12000 cm^{-1}). It is equipped with two different Fourier transform spectrometers, one for spectroscopy and one for spectromicroscopy. The microscope was removed from the beamline in September 2011 and is now in use at the new IR microscopy beamline D7 on MAX III.

The remaining spectrometer is a Bruker HR 120 which is used for high resolution, 0.001 cm^{-1}, spectroscopy. The setup has several options for introducing gases, liquids and solid samples. A gas cell, usable between 90 and 300 K, with a variable optical path length (maximum 120 m) is connected to the spectrometer.

MAX II Beamlines

The MAX II storage ring is equipped with three planar undulators and one elliptically polarizing undulator (EPU) for the VUV and soft X-ray regions and three multi-pole wigglers for the X-ray region. One conventional multi-pole wiggler beamline is used for powder diffraction. Of the two superconducting multi-pole wigglers, one is used for a materials science beamline for absorption and diffraction experiments (I811) and the other (I911) is used for a system of five independent beamlines mainly for protein crystallography and small angle X-ray scattering. The undulators serve beamlines with a variety of spectroscopic techniques such as X-ray absorption (including circular dichroism), X-ray emission, X-ray photoelectron spectroscopy and photoemission electron microscopy in the VUV and soft X-ray regions. A fourth spectroscopy beamline is installed on a bending magnet port where circularly polarized radiation can be used. A bending magnet beamline is also used for time resolved X-ray diffraction.

Beamline I311 is an undulator based VUV, soft X-ray beamline for high resolution X-ray photoemission spectroscopy (XPS) and X-ray absorption spectroscopy (XAS) and photo-

Table 2.
MAX II Beamlines

Beam port	Source type	Beamline / Monochromator	Energy or wavelength range	Experimental techniques
I311	Undulator	PGM (modified SX-700 with spherical focusing mirror)	43 - ~1500 eV	High resolution XPS. X-ray absorption spectroscopy. Photoemission electron microscopy, PEEM.
I411	Undulator	PGM (modified SX-700 with plane-elliptical focusing mirror).	40 - ~1500 eV	High resolution XPS. X-ray absorption spectroscopy. Coincidence spectroscopy.
I511/1	Undulator	PGM (modified SX-700 with spherical focusing mirror).	50 - ~1500 eV	High pressure XPS. X-ray absorption spectroscopy.
I511/3	Undulator	PGM (modified SX-700 with spherical focusing mirror).	50 - ~1500 eV	X-ray absorption spectroscopy. X-ray emission spectroscopy. Non-UHV compatible.
D611	Bending magnet	Be-windows, Double-crystal monochromator.	2 - 10 keV	Time resolved X-ray diffraction.
I711	Multi-pole wiggler	Be-window, Bent Si(111) crystal.	0.96 - 1.4 Å	Powder diffraction. Also used for SAXS until April 2011.
I811	Superconducting multi-pole wiggler	Double-crystal monochromator. Exchangable Si(111) & Si(311) crystals.	2 - 20 keV	EXAFS, XANES. Surface, interface and thin film crystallography.
I911/1	Superconducting multi-pole wiggler	Diamond crystal, multi-layer mirror.	Quasi-fixed wavelength, 1.2 Å	Presently used for education / test station.
I911/2	Superconducting multi-pole wiggler	Bent Si crystal, multi-layer mirror.	Fixed wavelength, 1.04 Å	Protein crystallography.
I911/3	Superconducting multi-pole wiggler	Collimating mirror. Double-crystal monochromator. Focusing toroidal mirror.	0.7 - 2.0 Å	Protein crystallography. MAD technique.
I911/4	Superconducting multi-pole wiggler	Bent Si crystal, multi-layer mirror.	Fixed wavelength, 0.91 Å	SAXS.
I911/5	Superconducting multi-pole wiggler	Diamond crystal, multi-layer mirror.	Fixed wavelength, 0.9 Å	Protein crystallography and other scattering experiments.
I1011	Undulator with variable polarization	Collimated PGM	200 - 2000 eV	MCD and related techniques for studies of magnetic materials.
D1011	Bending magnet	PGM (modified SX-700 with plane-elliptical focusing mirror). Off-plane radiation for circular polarized radiation.	40 - ~1600 eV	High resolution XPS. X-ray absorption spectroscopy. Circular dichroism.

emission electron microscopy (PEEM). The monochromator is a modified SX-700 type PGM with spherical optics and a movable exit slit. The source is a planar undulator with 48 periods and a period length of 54.4 mm covering the energy range from 43 eV up to about 1500 eV.

The main experimental station consists of separate analyser and preparation chambers accessible via a long-travel manipulator. The preparation chamber includes the usual equipment for preparation and characterization of surfaces (ion sputtering gun, LEED optics etc.). A hemispherical electron energy analyser (SCIENTA SES200) is used for photoelectron spectroscopy and XAS in Auger yield mode.

A SPELEEM instrument for photoemission electron microscopy is installed downstream from the main experimental station. This microscope has a spatial resolution better than 10 nm in the LEEM mode and 30 nm in the PEEM mode. It can also perform energy filtered XPEEM with a bandwidth of 300 meV in imaging mode, routinely achieving a lateral resolution of 30 nm.

Beamline I411 is based on an SX-700 type PGM and an undulator source (43-period, 59 mm period length) that covers the photon energy range 40 eV to about 1500 eV. The end-station has the unique versatility of being able to handle solid, liquid and gaseous samples. Thus the beamline is well suited for high-resolution electron spectroscopy on free atoms and molecules as well as for studies of liquids and non-UHV compatible solids.

The experimental system consists of separate analyser and preparation chambers accessible via a long-travel manipulator. The analyser chamber is equipped with a hemispherical electron energy analyser (SCIENTA R4000) which can be rotated around the incoming beam for polarization dependent measurements. In front of the experimental station a one-meter long section of the beamline can host other types of equipment for atomic and molecular spectroscopy, e.g. ion-electron coincidence detectors. A laser system for two-colour experiments is also available.

Beamlines I511/1 and I511/3 are used for XAS, XPS, and X-ray emission spectroscopy (XES) in the VUV and soft X-ray range. The two beamlines utilize a common undulator and monochromator with a flip-mirror placed immediately after the exit slit to direct the radiation alternately into two experimental stations. The undulator has 49 periods and a 52 mm period length giving a photon energy range of 50 to about 1500 eV. The monochromator is the same type of modified SX-700 monochromator as used on beamline I311.
During 2011 the new end-station at I511/1 aimed at surface studies under near-ambient pressure conditions has been commissioned and brought into user operation. This station is equipped with a SPECS Phoibos 150 NAP analyser for XPS, and XAS in Auger yield mode. Experiments at pressures up to some mbar are carried out using a dedicated high pressure cell, which can be moved in and out of the analysis UHV chamber.

Beamline I511/3 is equipped with a grazing incidence grating spectrometer for XES and can handle non-UHV compatible solids. The analysis chamber can be rotated around the incoming beam which makes it possible to utilize the linear polarization of the radiation.

Beamline D611 is a bending magnet beamline dedicated to time-resolved laser-pump/X-ray probe experiments. We are exploiting the fact that MAX II is a pulsed source operating at 100 MHz. The duration of the pulses has been measured to be approximately 350 ps using a streak camera. The beamline has a toroidal focusing mirror and a double crystal monochromator. A laser providing pulses with durations of 20-30 fs has been synchronised to the ring, and a streak camera yielding a temporal resolution of about 500 fs is available. The temporal resolution in the experiments does not depend on the relative jitter between the laser and the synchrotron (10 ps) but mainly on the jitter between the streak camera and the laser. The laser operates at a maximum repetition rate of 10 kHz which sets the data accumulation rate. Experiments can be performed in air or in vacuum (10^{-6} mbar). More information about these activities can be found at: *http://www.atomic.physics.lu.se/research/ultrafast_x_ray_science/.*

Beamline I711 has been used for powder diffraction during 2011 and also for SAXS during the first quarter of 2011. The SAXS experiments were then moved to the new set-up on beamline I911-4. I711 utilizes a 13-period, 1.8 T, multipole-wiggler and is designed to operate in the 0.8 Å (15.5 keV) to 1.6 Å (7.8 keV) region. The beamline has a vertical focusing mirror and a focusing single crystal monochromator working in the horizontal plane. This design sacrifices easy tunability and high energy resolution for high flux at the sample. The experimental station includes a 4-circle diffractometer with kappa geometry and a large area CCD detector.

Beamline I811 is used for X-ray absorption spectroscopy (EXAFS and XANES) and X-ray diffraction (XRD) experiments. It is based on a super-conducting multi-pole wiggler insertion device that produces high-flux photons in the energy range 2.4 - 20 keV (0.6 - 5 Å). The design is based on adaptive optics where the beam is collimated and focused vertically by cylindrical bendable first and second mirrors, respectively. Horizontal focusing is obtained by sagittal bending of the second monochromator crystal. The typical flux in a 1 x 1 mm^2 beam spot on the sample is 5 x 10^{11} photons/sec. One experimental station is used for XAS research with detectors for transmission and fluorescence yield techniques. A second station is equipped with a diffractometer for surface, interface and thin-film crystallography.

Beamline I911 is used mainly for macromolecular crystallography and SAXS but also some other diffraction experiments and for courses. The beamline receives radiation from a superconducting multi-pole wiggler and the wide fan of radiation is shared between five independent branch lines. The central part of the wiggler beam passes through a standard double-crystal monochromator set-up while the four side stations (two on each side) operate at fixed wavelengths. The optics for the side stations consists of horizontally focusing monochromator crystals and vertically focusing curved multilayer mirrors providing fixed wavelength beams. The side stations I911-1 and I911-5 are presently used as test set-ups.

MX beamlines I911-2 and I911-3
The side station I911-2 (wavelength 1.04 Å) is equipped with a single axis diffractometer and a 165 mm CCD detector. The central beamline I911-3 is tuneable in the range 0.75 - 2.0 Å and is optimized for MAD experiments. The beam is vertically collimated by a Rh-coated mirror, monochromatised by a Si(111) double-crystal monochromator and focused by a Rh-coated toroidal mirror. I911-3 is equipped with a microdiffractometer, a mini-kappa, a large-capacity automatic sample changer and a 225 mm CCD detector.

SAXS beamline I911-4
The new SAXS station, I911-4, has a fixed wavelength beam (0.91 Å) and is currently equipped with a mar165 detector. The accessible q-range is typically 0.01 - 0.3 $Å^{-1}$ but it can be extended by changing the set-up. The beamline offers different sample environments and it is also possible to install set-ups brought by the users in the easy accessible experimental "mini-hutch".

The beamline was taken in user operation in May 2011 and has attracted users from diverse fields of research performing measurements on biological macromolecules and membranes in solutions; natural and synthetic polymers; amorphous and crystalline solids, liquids, gels or powders, colloids and nanoparticles.

Beamline D1011 is a bending magnet beamline covering the energy range 40 to 1600 eV. An adjustable local bump of the electron beam provides out of plane radiation. This makes magnetic circular dichroism (MCD) possible in addition to photoemission and photoabsorption using linearly polarized light.

The monochromator is a modified SX-700 PGM of the same design as the monochromator on beamline I411. The experimental system consists of separate analyser and preparation chambers accessible via a long-travel manipulator. The analyser chamber is equipped with a SCIENTA SES200 electron energy analyser (with a lens of SES2002 type) and an MCP detector for electron yield measurements. The preparation chamber is equipped with LEED, ion sputtering guns, gas-inlet system and a number of optional ports for user owned sample preparation accessories.

A second experimental station receives radiation that is let through the first station and re-focused by a KB mirror system. This station is specifically designed for NEXAFS, XMCD and soft X-ray reflectivity experiments. Measurements can be performed under static magnetic fields of up to 500 G. One of the unique features of the station is to offer element specific reflection-based hysteresis measurements.

Beamline I1011 is used for studies of magnetic materials using MCD and related techniques. An EPU, with variable polarization (linear and circular), in the energy range 200 to 2000 eV is the source of the soft X-rays. The undulator radiation is monochromatised by an SX-700-type of PGM with vertical collimation and focused into an experimental chamber for MCD measurements.

There are currently two different chambers available to users. One being a chamber equipped with an octupole magnet allowing for work under applied magnetic fields in an arbitrary direction in space with, presently, a field of 0.6 T. The chamber is also designed to conduct soft X-ray magnetic reflectivity measurements. The second experimental system consists of separate preparation and analysis chambers. The analysis chamber is equipped with an UHV electromagnet providing a peak field of 0.1 T in pulsed mode and 35 mT with a continuous field. The preparation chamber is equipped with a LEED and an ion sputter gun as well as a number of extra ports for user supplied auxiliary equipment.

MAX III Beamlines

Two undulator beamlines are operational at the 700 MeV MAX III storage ring; one EPU covers the low energy region 5 - 50 eV and a planar undulator covers the energy range 13 - 200 eV. The undulators serve beamlines for angular and spin resolved photoelectron spectroscopy. A third beamline for infra-red microspectroscopy, utilising bending magnet radiation, is under commissioning.

Beamline I3 is an undulator beamline for the low energy region (5 - 50 eV). It is equipped with a normal incidence monochromator with a very high energy resolution (resolving power greater than 10^5). The undulator is of the "apple-type" providing variable polarization. There are two branch-lines, one with a fixed end-station for high resolution angle- and spin-resolved photoemission on solids, equipped with a rotatable Scienta R4000 analyser and a Scienta 2D spin detector. Angle resolved photoemission can be made in ±15, ±7 and ±3.5 degree mode. An on-line Molecular Beam Epitaxy (MBE) system provides the possibility for studying *in-situ* grown samples. The second branch-line, with a differential pumping stage, is designed for an easy exchange of end-stations for atomic and molecular spectroscopy and luminescence measurements.

Beamline I4 is an undulator beamline used for angle resolved photoemission. It is equipped with a spherical grating monochromator covering the energy range 13 to 200 eV. The end station analyser chamber hosts two electron energy analysers: An in vacuum rotatable VG ARUPS 10 analyser and a fixed mounted PHOIBOS 100 mm CCD analyser from SPECS. The SPECS analyser has an ultimate resolution of less than 3 meV. There are three angular dispersion modes namely MAD (medium angular dispersion), LAD (low angular dispersion) and WAM (wide angular dispersion). The MAD mode has angular acceptance of ±3 degrees with angular resolution of less than 0.1 degrees. The LAD mode has angular acceptance of ±6 degrees with angular resolution of about 0.15 degrees. The WAM mode has angular acceptance of ±10.5 degrees with angular resolution of about 0.4 degrees.

Beamline D7 is an infrared microspectroscopy beamline presently under commissioning. It receives radiation from a bending magnet port. A Bruker 66v/S spectrometer along with a Hyperion 3000 microscope is used for chemical imaging and mapping with a spatial resolution down to the diffraction limit. A 128 x 128 element focal plane array detector is available for fast image acquisition. The microscope can operate both in transmission and reflection mode. Additional objectives for gracing angle and ATR measurements are available as well. ■

Table 3.
MAX III Beamlines

Beam port	Source type	Beamline / Monochromator	Energy or wavelength range	Experimental techniques
I3	Undulator with variable polarization.	6.65 m Off-axis Eagle Type NIM.	5 - 50 eV	High resolution (meV) angle- and spin-resolved photoemission on solids. On-line MBE system.
I4	Undulator	5.5 - 5.8 m-SGM, 162°.	13 - 200 eV	Angle-resolved photoemission.
D7	Bending magnet	Transfer optics, FTIR spectrometer and IR microscope.	12000 - 10 cm^{-1}	Infrared microspectroscopy.

THE ASSOCIATION FOR SYNCHROTRON LIGHT USERS AT MAX-lab – FASM

The 24th annual meeting of “Föreningen för Användare av Synkrotronljuset vid MAX-laboratoriet, FASM” (The Association for Synchrotron Light Users at MAX-lab) took place in connection with the Annual User Meeting on November 14th, 2011 at hotel Scandic Star in Lund. During this meeting a new organisation, Swedish Synchrotron Radiation Users Organisation, SSUO, was founded with the goal to promote the interests of Swedish synchrotron light users in general, and as the Swedish representative in the European Synchrotron Radiation Users Organisation, ESUO. Olle Björneholm, UU, Jodie Guy, KI, Mats Fahlman, LiU, Torbjörn Gustafsson, UU, and Derek Logan, LU, were elected as members of the board of SSUO.

All users of the MAX-lab facility are by definition members of the FASM organisation. FASM aims at a broad participation involving all parts of the user community and at efficient communication with the MAX IV Laboratory board and management. It is thereby possible to communicate current and future needs within the user community and with the board and management. At the same time the association disseminates information to the users about the MAX IV plans and prospects. FASM’s mission is increasingly important as the user community is growing rapidly and more scientific disciplines are actively using the present MAX-lab facility, and even more so for the upcoming MAX IV facility. In view of this, FASM will introduce a number of proposals aimed at strengthening the activities at MAX-lab, deepening the knowledge of the possibilities at the new MAX IV facility and furthering the aid to new users by the association.

MAX-lab users and anyone with interest in using the MAX IV facility, who want to bring up ideas to improve MAX-lab as scientific tool and MAX IV as organisation are welcome to contact:

Professor Ingmar Persson
Department of Chemistry
Swedish University of Agricultural Sciences
P.O. Box 7015
SE-750 07 Uppsala, Sweden
E-mail: Ingmar.Persson@slu.se







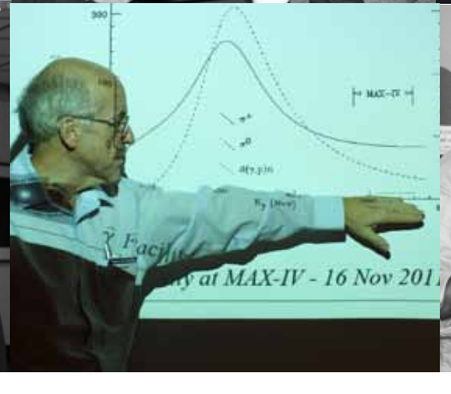

FACTS AND FIGURES

The budget of the MAX IV Laboratory is divided into two separate parts, one for the operation of the MAX-lab facility and the other for the construction of MAX IV as described earlier in this report. The operation budget for MAX-lab was 108 MSEK in 2011. The majority of the Funding (80 MSEK) was provided by the Swedish Research Council, while the host institution Lund University covered the rent, electricity and water costs which amounted to 28 MSEK.

The growth in the number of employees shown in Figure 1 is due to both the initiation of the MAX IV project mid-2010 and a strengthening of the support to users of MAX-lab. Though some staff members are dedicated exclusively to the MAX IV project the majority of the staff is engaged both in the operation of MAX-lab and the MAX IV. The staff is becoming more and more international, at the beginning of 2012 13 nationalities were represented among the laboratory staff.

The scientific highlights presented previously in this report could not have been achieved without the good performance of the MAX-lab accelerators described in the chapter *MAX-lab Rings and Accelerators*. The availability of radiation from MAX II and MAX III to the users has improved significantly in 2011 compared to 2010 (Figure 2).

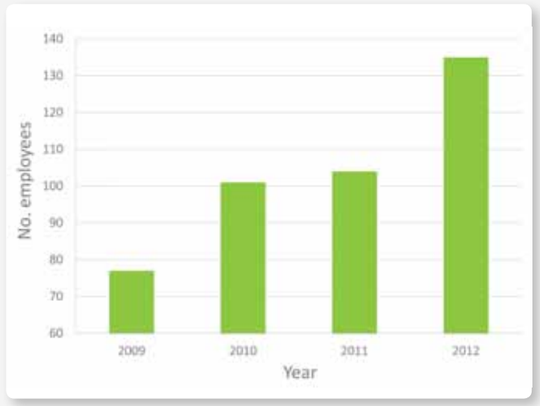

Figure 1.
Number of employees at the MAX IV Laboratory. Presented figures are end of the year data (the 2012 figure is an estimate for August 2012).

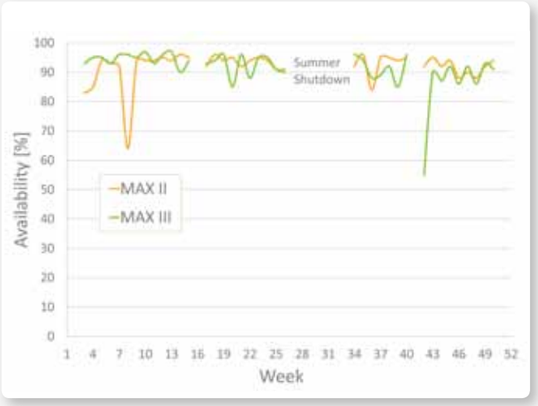

Figure 2.
Weekly availability of MAX II and MAX III to users during 2011.

MAX-lab Users

The number of proposals submitted for beamtime continues to increase and in 2011 more than 370 applications were received requesting about twice the amount of available beamtime (Figure 3 and Figure 4). Proposals are reviewed by the MAX IV Program Advisory Committees (PAC), who also recommends the amount of allocated beamtime. Research performed at MAX-lab resulted in the publication of more than 180 research papers in 2011.

During 2011 more than 900 scientists performed experiments at MAX-lab. The scientific projects included experiments in atomic and molecular physics, solid state physics, surface physics, material science, chemistry, life science and environmental science. The majority of the experiments have been performed on the MAX II and MAX III storage rings. The researchers represented 160 different industrial, academic and government laboratories from 35 different countries (Figure 5). The number of visiting researchers follows the strong trend, observed over more than twenty years, of an expanding MAX-lab user community (Figure 6).

Table 1.

MAX IV Laboratory Program Advisory Committee (PAC)

Lars Johansson (chairperson), Karlstad University, Sweden

Soft X-ray and IR science
Anne Borg, Norwegian University of Science and Technology, Norway
Nicholas Brookes, ESRF, France
Carol Hirschmugl, University of Wisconsin–Milwaukee, USA
Karsten Horn, Fritz-Haber-Institut der Max-Planck-Gesellschaft, Germany
Maya Kiskinova, ELETTRA, Italy
Edwin Kukk, University of Turku, Finland
Catalin Miron, SOLEIL, France
Luc Patthey, PSI, Swiss Light Source, Switzerland
Wilfried Wurth, University of Hamburg, Germany
Wendy Flavell, The University of Manchester, UK

X-ray science
Jean Daillant, SOLEIL, France
Andrew N. Fitch, ESRF, France
Mikael Gajhede, University of Copenhagen, Denmark
Bill Hunter, University of Dundee, UK
Ragnvald Mathiesen, Norwegian University of Science and Technology, Norway
Henning Friis Poulsen, Risø-DTU, Denmark

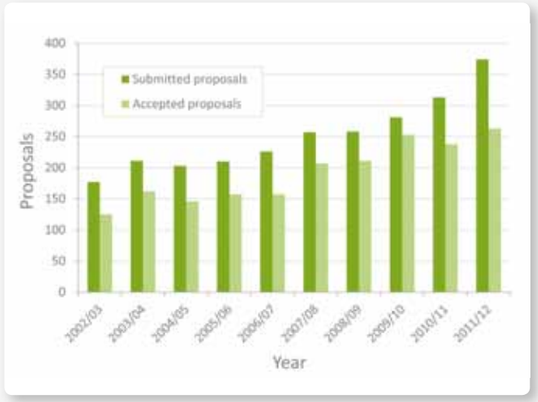

Figure 3.
Number of submitted and approved proposals for beamtime at MAX I, II and III per year.

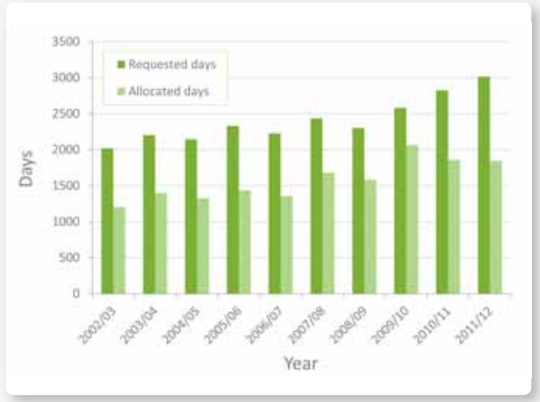

Figure 4.
Requested and allocated beamtime at MAX I, II and III per year.

Organisation of the MAX IV Laboratory

The MAX IV Laboratory was created through an agreement between Lund University, Swedish Research Council, VINNOVA and Region Skåne, which was signed in the fall of 2010. The creation of the MAX IV Laboratory has been accompanied by organisational changes.

The overall responsibility for the laboratory resides with the Board chaired by Lars Börjesson as shown in Table 2. The Forum for Funders (Table 3) holds the overall responsibility for the development and financial aspects of the MAX IV project.

Table 2.

MAX IV Laboratory Board

Lars Börjesson (chairperson), Chalmers University of Technology, Sweden
Helmut Dosch, DESY, Germany
Kristina Edström, Uppsala University, Sweden
Lars Hultman, Linköping University, Sweden
Anne l'Huillier, Lund University, Sweden
Sine Larsen, Copenhagen University, Denmark (until 15 February 2011)
Gunter Schneider, Karolinska institutet, Sweden
Stacey Sörensen, Lund University, Sweden
Ingrid Reineck, Sandvik AB, Sweden (until 1 July 2011)
Michel van der Rest, ESRF Council, France (from 17 November 2011)
Maria Åstrand, Sandvik AB, Sweden (from 17 November 2011)

Table 3.

Forum for Funders

Lars Börjesson (chairperson), MAX IV Laboratory Board
Sven Strömqvist, Lund University
Harald Lindström, Region Skåne
Eva Lindencrona, VINNOVA
Lars Kloo, Swedish Research Council
Johan Holmberg, Swedish Research Council
Sine Larsen, MAX IV Laboratory (observer)
Peter Andersson, MAX IV Laboratory (observer)
Lise Bröndum, Lund University (observer)

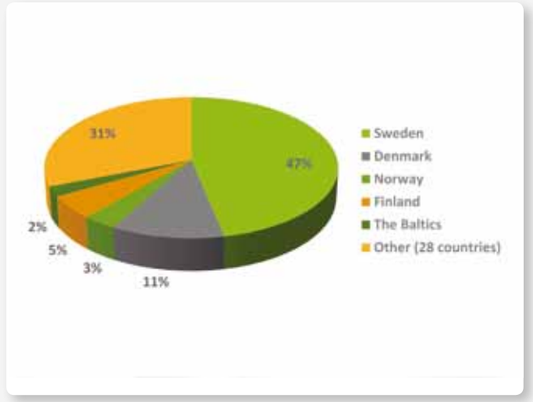

Figure 5.
Allocated beamtimes versus origin of the approved proposals for the year 2011.

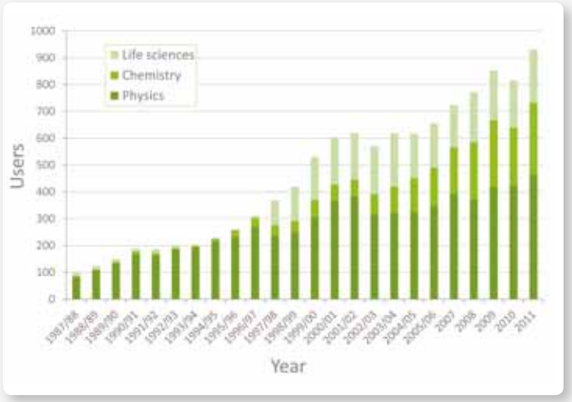

Figure 6.
Number of MAX I, II and III users per year and discipline. The 1987/88 to 2004/05 numbers are July to June figures. The 2005/2006 value indicates number of users from June 2005 to end of 2006.

The operation of the MAX IV Laboratory is led by the management team comprised of the Director of the laboratory, the Science Director, the Machine Director and the Administrative Director. During 2011 and early 2012 an overall line organisational structure for the laboratory (Figure 7) was put in place. As almost all the work involved with MAX IV is organised in projects a separate project structure has also been created (Figure 8). Together the line and project structure form a matrix organisation of the work of the MAX IV Laboratory.

Table 4.

MAX IV Laboratory Managerial Group

Sine Larsen, Director *
Mikael Eriksson, Machine Director
Jesper Andersen, Science Director
Peter Andersson, Administrative Director

** Succeeded by Christoph Quitmann in August 2012*

The Machine Advisory Committee (MAC) and Science Advisory Committee (SAC) both provide valuable advice to the Management and Board of the MAX IV Laboratory. The composition of the SAC and MAC is listed in Table 5 and 6.

Table 5.

MAX IV Laboratory Scientific Advisory Committee (SAC)

Börje Johansson (chairperson), Uppsala University and Royal Inst of Technology, Sweden
Rafael Abela, PSI, Swiss Light Source, Switzerland
Helena Aksela, University of Oulu, Finland
Wolfgang Eberhardt, HZB, Germany
Giorgio Margaritondo, EPFL, Switzerland
Lynne McCusker, ETH-Zürich, Switzerland
Alfons Molenbroek, Haldor Topsoe A/S, Denmark
Harald Reichert, ESRF, France
Ian Robinson, London Center for Nanotechnology, UK
Gebhard Schertler, PSI, Swiss Light Source, Switzerland
Phil Woodruff, University of Warwick, UK

Table 6.

MAX IV Laboratory Machine Advisory Committee (MAC)

Lenny Rivkin (chairperson), PSI, Swiss Light Source, Switzerland
Klaus Balewski, DESY, Germany
Peter Kuske, Institute Accelerator Physics, HZB, Germany
Søren Pape Møller, Institute for Storage Ring Facilities, Aarhus University, Denmark
Richard Walker, Diamond, UK
Bob Hettel, SLAC, USA

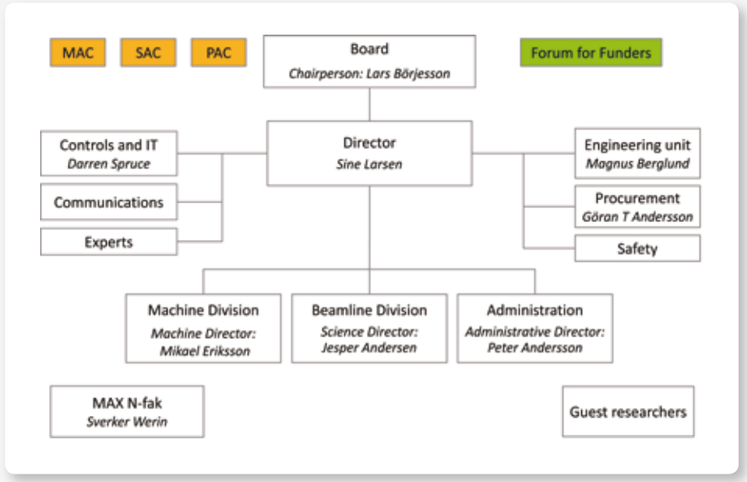

Figure 7.
MAX IV Laboratory line organisation.

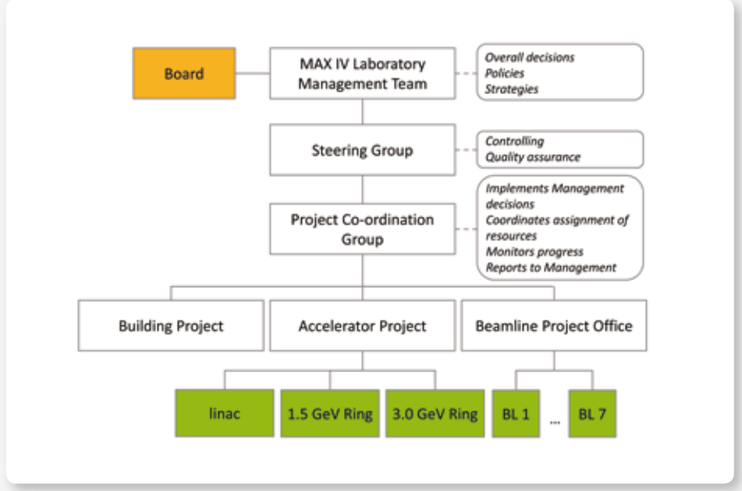

Figure 8.
MAX IV project organisation.

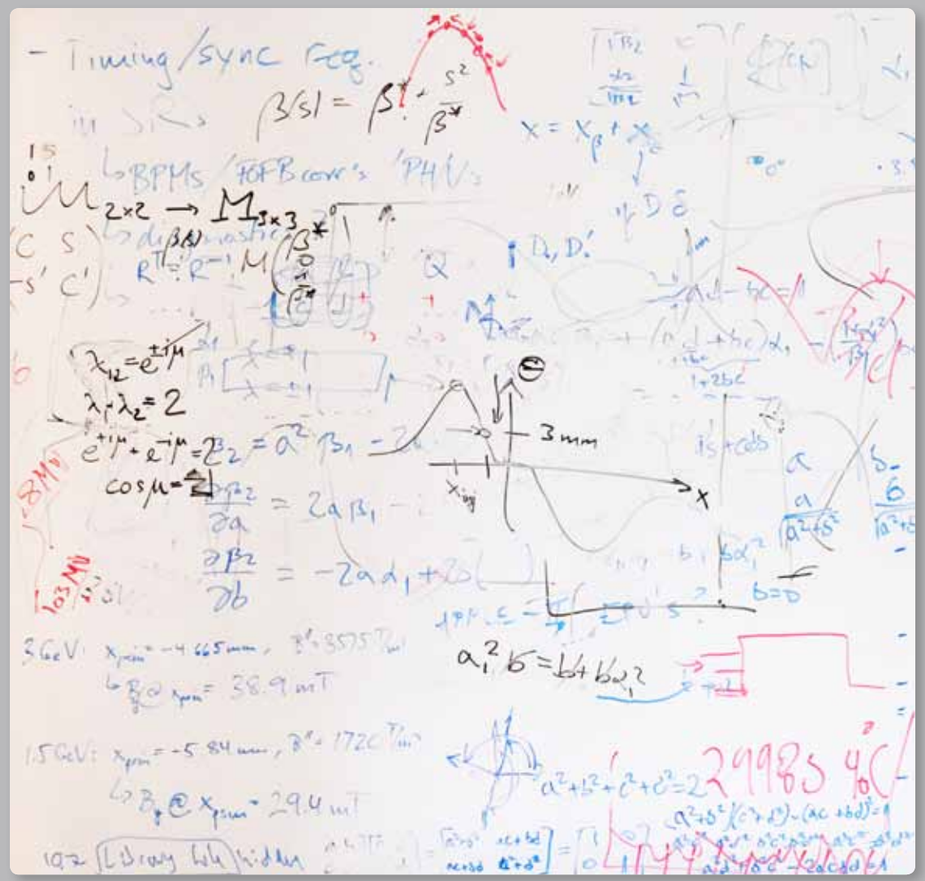

Contributors

Patrik Almqvist
Jesper Andersen
Peter Andersson
Åke Andersson
Mikael Eriksson
Franz Hennies
Brian Norsk Jensen
Sine Larsen
Andreas Lassesson
Lars Lavesson
Karin Lilja
Caj Lundquist
Annika Nyberg
Ralf Nyholm
Ingmar Persson
Cecilia Sturén
Pedro Fernandes Tavares
Helena Ullman
& All the authors of the Scientific Highlights

Editor: Sine Larsen
Design: Borstahusen Kommunikation AB
Print: CA Andersson
Paper: Cover Arctic Volume White 300 g, insert Arctic Volume White 130 g.
Photos: El Sayed El Afifi, Lasse Davidsson, Perry Nordeng, Annika Nyberg, Johan Persson, Bengt-Erik Wingren, Mostphotos.
Illustrations: Borstahusen, FOJAB arkitekter and Snøhetta, Johnny Kvistholm, Andreas Lassesson, Cecilia Sturén, authors of the Scientific Highlights.

MAX IV Laboratory
Lund University
P.O Box 118
SE-221 00 Lund
Sweden

Tel: +46 (0)46 222 98 72
www.maxlab.lu.se

MAX IV
LABORATORY